Prepared for submission to JHEP

Born-Oppenheimer Renormalization group for High Energy Scattering: the Modified BFKL, or where did it all go?

Haowu Duan,[a] **Alex Kovner**[a,b] **and Michael Lublinsky**[c]

[a] *Physics Department, University of Connecticut, 2152 Hillside Road, Storrs, CT 06269, USA*

[b] *ExtreMe Matter Institute EMMI, GSI Helmholtzzentrum fuer Schwerionenforschung GmbH, Planckstrasse 1, 64291 Darmstadt, Germany*

[c] *Physics Department, Ben-Gurion University of the Negev, Beer Sheva 84105, Israel*

Abstract: We continue exploring the Born-Oppenheimer renormalization group generating evolution in frequency of physical observables. In this paper we study the evolution of the total cross section for dilute-dilute scattering retaining only eikonal emissions. We derive and analyze the analog of the BFKL equation in this framework. The frequency evolution has a very strong effect on the solutions of the BO-BFKL equation, slowing down the evolution of the scattering amplitude in a spectacular fashion: the intercept of the Pomeron is decreased by about a factor of three relative to the canonical LO BFKL result. The anomalous dimension is also modified significantly - from the BFKL value of one it goes down to the negative value of ≈ -0.2. Introducing saturation boundary as a proxy for the full saturation dynamics, we find that the dependence of the saturation momentum on rapidity η becomes quite weak with $Q_s^2 \sim e^{a\bar{\alpha}_s\eta}$ with $a \approx 0.784$ as opposed to the BFKL value $a = 4.88$. Our results underscore the necessity to take into account the DGLAP effects in the high energy evolution. This is left for future work.

Contents

1 Introduction

This is the third paper in the series dealing with the Born-Oppenheimer (BO) renormalization group approach to quantum evolution in QCD. In the previous papers [1, 2] we formulated the BO approximation for the light cone wave function (LCWF) $|\Psi_P\rangle$ of a fast moving projectile hadron with longitudinal momentum P^+ and initiated the study of evolution based on the sequence of BO approximations (k^- ordering) for increasingly higher frequency modes. The parameter of this evolution is the frequency E (or rather "rapidity" $\eta = \ln \frac{E}{E_0}$) which limits the frequency of "resolved" gluons allowed in the wave function.

This approach relies on the intuition that in a physical process in which the time of interaction with the target is short, the target can only resolve the modes of the projectile gluon field which do not fluctuate on this time scale. In terms of a physical process (or interesting observable) this time scale can have different meaning. For example in the high energy scattering where one measures the total cross section, this time scale is determined by the "Ioffe time" - which is the time during which a fast projectile particle traverses over the full longitudinal extent of the target. In DIS on the other hand, the time scale is determined by the interaction time with a short lived highly virtual photon, and therefore by the momentum transfer Q^2. Thus the BO evolution is a versatile tool in the sense that the physical meaning of the evolution parameter can be adapted to the physical process/observable of interest.

In [2] we studied in detail the BO evolution of "partonic" observables, i.e. gluon TMD and PDF. We have shown that, at intermediate x, the BO evolution leads to the standard perturbative evolution equations - CSS for TMD [3–6], and DGLAP for PDF, amended by the higher twist nonlinear corrections. The nonlinear corrections in question have the natural interpretation of stimulated gluon emission. Interestingly, these corrections turn out to be negative for PDF, so that their effect mimics to some degree that of saturation, even though the physics is quite different. At small x we also found corrections to the DGLAP equation which stem from the BFKL like kinematics of splittings. These corrections effectively lead to increasing the transverse resolution scale on the RHS of the DGLAP equation. For these observables the role of the evolution parameter E is to determine the transverse, Q^2 and longitudinal, ζ resolution scales that are necessary to define the TMD and PDF.

In [2] we were interested in values of the gluon's longitudinal momentum $k^+ = xP^+$ and transverse momentum $\boldsymbol{k}$ which generically are far away from the kinematic boundaries on these quantities imposed by the value of the evolution parameter E, so that additional lower x and higher $\boldsymbol{p}$ gluons are present in the LCWF.

However our original motivation for developing the BO approach was to understand/resum large perturbative corrections to NLO JIMWLK evolution [7–21]. The problems with high energy evolution beyond leading order are not new, and have been studied in the context of the linear BFKL equation a while ago [22–31]. The issues here are associated with energy non conservation in leading order (LO) BFKL equation as well as with DGLAP type corrections which lead to appearance of large transverse logarithms at NLO. The same problems have been inherited by the NLO JIMWLK evolution and have been numerically seen a long time ago [32]. Several proposals were made over the years of how to resum the large logs by limiting the phase space of low x emissions on one hand [31, 33–37], and taking care of the missing piece in the gluon splitting function on the other [38]. The first approach is meant to take care of corrections associated with energy conservation, while the second with missing DGLAP emissions.

In this paper we return to our original motivation, and study the analog of the BFKL equation as it arises in the BO approach*. The S-matrix for scattering on a dilute target in the $A^+ = 0$ gauge is given by† (see [1])

$$S = 1 - \frac{1}{2(N_c^2-1)} \int_q \langle \Psi_T | \gamma_j^{\dagger b}(q) \gamma_j^b(q) | \Psi_T \rangle \, O(q) \tag{1.1}$$

where γ is the target field, $\langle \Psi_T | \gamma_j^{\dagger b}(q) \gamma_j^b(q) | \Psi_T \rangle$ denotes the average over the target wave function (ensemble of fields), and O is the matrix element in the projectile Hilbert space

$$O(q) = \langle \Psi_P | \mathcal{C}_i^a(q^-, \boldsymbol{q}) \mathcal{C}_i^{a\dagger}(q^-, \boldsymbol{q}) | \Psi_P \rangle_E; \tag{1.2}$$

$$\mathcal{C}_i^{a\dagger}(q^-, \boldsymbol{q}) = g \int_{k:k^-<q^-} f_{lk}^i(k,q) A_l^\dagger(k^+, \boldsymbol{k}+\boldsymbol{q}) T^a A_k(k^+, \boldsymbol{k}) \tag{1.3}$$

Here $A_i^a(k) \equiv \frac{1}{\sqrt{2k^+}} \hat{a}_i^a(k)$; $\quad A_i^{a\dagger}(k) \equiv \frac{1}{\sqrt{2k^+}} \hat{a}_i^{a\dagger}(k)$, with $\hat{a}^\dagger$ and $\hat{a}$ – projectile's gluon creation and annihilation operators. The fields satisfy the canonical light cone commutation relation

$$[A_i^a(p), A_j^{b\dagger}(q)] = (2\pi)^3 \delta_{ij}^{ab} \frac{1}{2p^+} \delta^3(p-q). \tag{1.4}$$

*Just like in the two previous papers we exclude quarks from consideration for simplicity.

†We use the shorthand notation $\int_k \equiv \int \frac{d^2\boldsymbol{k} dk^+}{(2\pi)^3}$.

The coefficient function in (1.2) is given by

$$f^i_{jk}(k,q) = 2k^+ \frac{\boldsymbol{q}^i}{\boldsymbol{q}^2}\delta^{jk} + 4k^+\epsilon^{il}\frac{\boldsymbol{q}^l}{\boldsymbol{q}^2}\epsilon^{jk}\frac{1}{\frac{2q^-k^+}{\boldsymbol{q}^2}-1}. \tag{1.5}$$

In (1.2) we assumed that the target field is monochromatic with transverse momentum $\boldsymbol{q}$ and frequency $q^- \sim E$. This assumption is easily relaxed if the target fields are distributed with a finite spread in momentum.

When the fields of the target are very soft, i.e. $q^- \gg \frac{\boldsymbol{q}^2}{2k^+}$ we recover the eikonal expression for the S-matrix. In this limit only the first term in (1.5) needs to be kept and we have

$$f^i_{lk}(k,q) \to 2k^+\frac{\boldsymbol{q}_i}{\boldsymbol{q}^2}\delta_{kl}; \qquad \mathcal{C}^{a\dagger}_i(q^-,q) \to \frac{\boldsymbol{q}_i}{\boldsymbol{q}^2}\rho^a(\bar{q}^+,\boldsymbol{q}); \qquad \bar{q}^+ \equiv \frac{\boldsymbol{q}^2}{2q^-} \tag{1.6}$$

with the color charge density

$$\rho^a(q^+,\boldsymbol{q}) = g\int_{k^+>q^+}\frac{dk^+}{2\pi}\frac{d^2\boldsymbol{k}}{(2\pi)^2}a^\dagger_i(k^+,\boldsymbol{k}+\boldsymbol{q})T^a a_i(k^+,\boldsymbol{k}) \tag{1.7}$$

The S-matrix then is given by the standard eikonal expression (expanded to leading order in the target fields).

In this paper we assume that the target indeed contains only small transverse momentum component fields, and therefore the scattering matrix is given by the eikonal expression. One has to realize that even if the scattering is on the soft target fields only, this still allows DGLAP type splittings in the evolution of the observable. These splittings in principle can strongly affect the evolution of the correlator of color charges which, as per (1.2),(1.6) is proportional to the scattering amplitude. Taking into account the effect of DGLAP splittings in the evolution is important and undoubtedly has to be done. In the present paper however we will not perform the complete analysis. Our goal here is only to understand how the frequency ordering in conjunction with the eikonal approximation affects the BFKL equation. Therefore to simplify the problem we will neglect the DGLAP contributions to evolution of the scattering matrix, and keep only the eikonal contributions in the whole phase space. This is not to say that we neglect emissions with strongly ordered transverse momenta altogether, but only keep that part which is both transverse momentum ordered and also eikonal. This means that in our calculation the DGLAP regime is approximated by the doubly logarithmic contributions.

Again we stress that the genuine DGLAP corrections are important and may be sizable. In the k^+ ordering scheme, the DGLAP corrections to the evolution have to be resummed separately inside the JIMWLK (or BFKL) Hamiltonian [38]. In the BO approach the situation is different and they appear directly in the LO calculation. We therefore expect that it is not prohibitively difficult to include them. In future publications we are planning to analyze the complete evolution. In the present paper however, we will only analyze the effects of rapidity (or k^-) ordering on the eikonal approximation. We note that in the k^+ ordering scheme, inclusion of the DGLAP corrections slows down the evolution, and we expect a similar effect in the BO framework, however this has to be verified by explicit calculations.

This paper is structured as follows. In Sec. 2 we derive the evolution equation for the color charge density correlator $\langle\rho\rho\rangle$ using eikonal splitting approximation in the whole phase space. As opposed to the standard BFKL/JMWLK approach, the color charge density $\rho(k^+,\boldsymbol{k})$, which represents the emission

vertex of a gluon with momentum k, is not assumed to be independent of the longitudinal momentum of the emitted gluon. Instead we respect the momentum conservation in the sense that the longitudinal momentum of the emitted gluon is restricted to be smaller than that of the emitter. This dependence on k^+ is important for the evolution. The resulting equation, which we dub BO-BFKL equation turns out to be very similar to the BFKL equation in the ultraviolet, but is significantly more regular in the infrared.

In Sec. 3 we discuss eigenfunctions of this equation. We find that the relevant eigenfunctions are still pure powers of transverse momentum $\boldsymbol{k}$; such that $f_\gamma = |\boldsymbol{k}|^\gamma$ as in the BFKL case, but the eigenvalue spectrum is significantly different. Whereas for the BFKL, the real part of the eigenvalue is limited by $0 < \mathrm{Re}(\gamma) < 2$, for the BO-BFKL the range is $-2 < \mathrm{Re}(\gamma) < 2$. Just like for the BFKL, at asymptotically large rapidities the correlator is dominated by a saddle point, but the saddle point is at a different value of γ. We calculate the eigenvalue spectrum numerically and find that the saddle point value is $\gamma_0^{BO} \approx -0.2$. This is a significant shift from the BFKL value $\gamma_0^{BFKL} = 1$. Correspondingly, the anomalous dimension is also shifted to this value so that the transverse momentum dependence of the color charge correlator at large η is given by $\langle \rho^a(\boldsymbol{k})\rho^a(-\boldsymbol{k})\rangle \sim |\boldsymbol{k}|^{-0.2}$. Perhaps most surprisingly, we find that the Pomeron intercept at large rapidity is about a factor of three smaller than for the BFKL, so that the growth of the cross section is much slower. Finally, we impose the saturation boundary on our evolution following [39], and find the saturation saddle point numerically. The resulting rapidity dependence of the saturation momentum is $Q_s^2|_{BO-BFKL} \sim \exp\{0.784\bar{\alpha}_s\eta\}$ to be compared with the BFKL value $Q_s^2|_{BFKL} \sim \exp\{4.88\bar{\alpha}_s\eta\}$.

All these effects are caused by the softening of the evolution in the infrared due to frequency ordering coupled with the energy conservation.

Finally in Sec. 4 we summarise our results.

2 The evolution of the scattering amplitude

In [1] we derived the light cone wave function (LCWF) of the projectile at high energy. The wave function of the system evolved from the initial frequency (energy) E_0 to the frequency E is given by

$$|\Psi_E\rangle = \mathcal{P}\exp\{i\int_{E_0}^{E} dp^- G(p^-)\}|\Psi_{E_0}\rangle \tag{2.1}$$

where $\mathcal{P}$ denotes path ordering along the frequency coordinate and

$$G(p^-) \equiv \int \frac{dp^+ d^2\boldsymbol{p}}{(2\pi)^3}\,\delta(p^- - \frac{\boldsymbol{p}^2}{p^+})G(p^+,\boldsymbol{p}^2); \tag{2.2}$$

with $G(p^+,\boldsymbol{p})$ given by

$$\begin{aligned} G(p^+,\boldsymbol{p}) = g\int_{k^-<p^-;\ (k-p)^-<p^-} & \frac{dk^+}{2\pi}\frac{d^2\boldsymbol{k}}{(2\pi)^2}A_i^a(k^+,\boldsymbol{k})\frac{2p^+(k^+-p^+)}{k^+} \\ \times \Bigg\{ & \left[\delta_{ki}\delta_{jl}\left(\frac{2k^+}{p^+}-1\right)+\epsilon_{ki}\epsilon_{jl}\right]\frac{\boldsymbol{p}_j}{\boldsymbol{p}^2}A_l^\dagger(p^+,\boldsymbol{p})T^aA_k^\dagger(k^+-p^+,\boldsymbol{k}-\boldsymbol{p}) \\ - & \left[\delta_{ki}\delta_{jl}\left(\frac{2k^+}{k^+-p^+}-1\right)+\epsilon_{ki}\epsilon_{jl}\right]\frac{\boldsymbol{p}_j}{\boldsymbol{p}^2}A_l^\dagger(k^+-p^+,\boldsymbol{k}-\boldsymbol{p})T^aA_k^\dagger(p^+,\boldsymbol{p})\Bigg\} + h.c. \end{aligned} \tag{2.3}$$

A convenient representation is

$$G(p^+,\boldsymbol{p}) = A_i^\dagger(p^+,\boldsymbol{p})C_i(p^+,\boldsymbol{p}) + A_i(p^+,\boldsymbol{p})C_i^\dagger(p^+,\boldsymbol{p}) \tag{2.4}$$

with

$$\begin{aligned} C_i^a(p^+,\boldsymbol{p}) =& g\int_{p^->k^-,p^->(k-p)^-} \frac{dk^+d^2\boldsymbol{k}}{(2\pi)^3}\frac{2p^+(k^+-p^+)}{k^+} \\ &\times\left\{\left[\delta_{kl}\delta_{ji}\left(\frac{2k^+}{p^+}-1\right)+\epsilon_{lk}\epsilon_{ji}\right]+\left[\delta_{ki}\delta_{jl}\left(\frac{2k^+}{k^+-p^+}-1\right)+\epsilon_{ik}\epsilon_{jl}\right]\right\} \\ &\times\frac{\boldsymbol{p}_j}{\boldsymbol{p}^2}A_l^\dagger(k^+-p^+,\boldsymbol{k}-\boldsymbol{p})T^aA_k(k^+,\boldsymbol{k}) \end{aligned} \tag{2.5}$$

The operator C in the BFKL regime, $p^+ \ll k^+$ reduces to the "classical field" produced by the slow modes. In the DGLAP regime, for $|\boldsymbol{p}|^2 \gg |\boldsymbol{k}|^2$ and $k^+ \sim p^+$, C contains one slow and one fast mode but we still find this form useful in calculations.

As a shorthand, it is convenient to introduce

$$\begin{aligned} F_{lk}^i(k,p) &= \frac{2p^+(k^+-p^+)}{k^+}\left\{\left[\delta_{kl}\delta_{ji}\left(\frac{2k^+}{p^+}-1\right)+\epsilon_{lk}\epsilon_{ji}\right]+\left[\delta_{ki}\delta_{jl}\left(\frac{2k^+}{k^+-p^+}-1\right)+\epsilon_{ik}\epsilon_{jl}\right]\right\}\frac{\boldsymbol{p}_j}{\boldsymbol{p}^2} \\ &= \frac{4p^+(k^+-p^+)}{k^+}\left\{\delta_{kl}\delta_{ji}\frac{k^+}{p^+}+\delta_{ki}\delta_{jl}\frac{k^+}{k^+-p^+}-\delta_{kj}\delta_{il}\right\}\frac{\boldsymbol{p}_j}{\boldsymbol{p}^2} \end{aligned} \tag{2.6}$$

such that

$$C_i^a(p^+,\boldsymbol{p}) = g\int_{k^-<p^-;\ \ (k-p)^-<p^-}\frac{dk^+}{2\pi}\frac{d^2\boldsymbol{k}}{(2\pi)^2}F_{lk}^i(k,p)A_l^\dagger(k^+-p^+,\boldsymbol{k}-\boldsymbol{p})T^aA_k(k^+,\boldsymbol{k}) \tag{2.7}$$

$$C_i^{a\dagger}(p^+,\boldsymbol{p}) = g\int_{k^-<p^-;\ \ (k+p)^-<p^-}\frac{dk^+}{2\pi}\frac{d^2\boldsymbol{k}}{(2\pi)^2}F_{kl}^i(k+p,p)A_l^\dagger(k^++p^+,\boldsymbol{k}+\boldsymbol{p})T^aA_k(k^+,\boldsymbol{k}) \tag{2.8}$$

As we mentioned in the Introduction, in this paper we only keep the BFKL type eikonal emissions in (2.1). Practically this means that we take the eikonal limit of the function F in (2.6) by assuming $p^+ \ll k^+$:

$$F_{lk}^i(k,p) = 4k^+\delta_{kl}\frac{\boldsymbol{p}_i}{\boldsymbol{p}^2} \tag{2.9}$$

so that

$$C_i^a(p^+,\boldsymbol{p}) \approx 4gk^+\frac{\boldsymbol{p}_i}{\boldsymbol{p}^2}\int_{k^-<p^-;\ \ (k-p)^-<p^-\ \ k^+>p^+-}\frac{dk^+}{2\pi}\frac{d^2\boldsymbol{k}}{(2\pi)^2}A_j^\dagger(k^+,\boldsymbol{k}-\boldsymbol{p})T^aA_j(k^+,\boldsymbol{k}) = \frac{2i\boldsymbol{p}_i}{\boldsymbol{p}^2}\rho^a(p^+,-\boldsymbol{p}) \tag{2.10}$$

Note that although we substitute $p^+ \ll k^+$ in (2.6), in (2.10) the momentum k is integrated over the whole momentum range $p^+ < k^+$ just as in the original BFKL calculation. The condition $p^+ < k^+$ is not an external restriction on the phase space, but is required by the momentum conservation, since an emitted particle must have a smaller longitudinal momentum than the emitter, no matter what is the probability of the emission. In this approximation we therefore do not impose any restrictions on the phase space of the emissions, but approximate the emission amplitude by its eikonal form. This is important to keep in

mind in view of our results. Thus our calculation should be equivalent to the BFKL eikonal evolution with an additional constraint on the frequency of the contributing modes.

Our aim now is to calculate the evolution of the correlator of color charge density ρ, since it is proportional to the scattering amplitude. We will be initially slightly more general, and calculate the evolution of the following operator

$$\hat{O} \equiv \rho^a(l^+, \boldsymbol{p})\rho^a(m^+, -\boldsymbol{p}) \tag{2.11}$$

without requiring $l^+ = m^+$. Without loss of generality we assume $l^+ \geq m^+$. We will restrict ourselves to the case $l^+ = m^+$ later, when analyzing the high energy behavior of the amplitude.

To derive the evolution equation for any operator $\hat{O}$ first consider the expectation value

$$\langle \hat{O} \rangle_E = \langle \Psi_P | \hat{O} | \Psi_P \rangle_E \tag{2.12}$$

with $|\Psi_P\rangle_E$ given by (2.1). To derive the differential form of the evolution we introduce an increment in energy, Ee^{Δ} for an infinitesimal Δ. The interval of momenta $E < p^- < Ee^{\Delta}$, which we will sometimes refer to as "the window", is the phase space opened by one small step in the evolution. The modes below E are the valence modes while the window is populated by the fast modes [1]. The change in the expectation value due to a single step in the evolution is

$$\delta\langle \hat{O} \rangle \equiv \langle \hat{O} \rangle_{Ee^{\Delta}} - \langle \hat{O} \rangle_E \tag{2.13}$$

The evolution is derived by expanding the exponential factor in (2.1) to second order in C_i and averaging over the Hilbert space of the fast gluons. Since the state $|\Psi_P\rangle_E$ is a vacuum of the fast modes in the window, $|\Psi_P\rangle_E = |0\rangle_F \otimes |\Psi_P\rangle_E$, we are able to explicitly average over these modes in calculating the expectation value.

In [2] we have calculated the evolution of the gluon TMD using this approach. The calculation here proceeds along similar lines, but with two new elements.

First, for the TMD the observable depends only on the gluon degrees of freedom that live below the window in rapidity opened by the last step of the evolution. For such observables, as discussed in [2] the evolution is given entirely by what we called, the Lindblad term

$$\begin{aligned}\delta\langle \hat{O} \rangle_{|_L} &= \int_{E<p^-<Ee^{\Delta}} \frac{d^3p}{(2\pi)^3}\frac{1}{2p^+}\langle C^\dagger(p)\hat{O}C(p) - \frac{1}{2}C^\dagger(p)C(p)\hat{O} - \frac{1}{2}\hat{O}C^\dagger(p)C(p)\rangle_E \\ &= \frac{1}{2}\int_{E<p^-<Ee^{\Delta}} \frac{d^3p}{(2\pi)^3}\frac{1}{2p^+}\langle \{C^\dagger(p)[\hat{O}, C(p)] + h.c.\}\rangle_E \end{aligned} \tag{2.14}$$

For the color charge correlator the Lindblad term does not exhaust all the contributions, since the observable $\hat{O}$ in (2.11) also depends explicitly on the gluon degrees of freedom in the window.

The second new element has to do with the fact that when calculating the scattering amplitude we have to account for the process where a particle in the window scatters with change in frequency such that after scattering it does not remain in the window, but rather ends up with the frequency smaller than E. As we will see such a contribution indeed arises, and affects nontrivially the evolution. This contribution is given by a term where only one of the wave functions in the calculation of the matrix element contains a correction due to emission of a new particle, while the other wave function is unevolved. We will call this contribution "the lopsided contribution" and will calculate it later.

We now calculate the different contributions to the evolution separately.

2.0.1 The Lindblad term

The contribution Eq.(2.14) exists also for operators that involve gluons in the window. It arises from one particular term where the operator $A^\dagger$ that multiplies the amplitude C is contracted directly with the operator A that multiplies $C^\dagger$, whereas all the gluon operators in the window contained in the observable $\hat{O}$ are contracted in the vacuum. This is the contribution due to scattering of gluons with energies $p^- < E$ that were present in the wave function before the last step in the evolution, but whose distribution has been changed due to emission of gluons with frequency E.

Since ρ^a as defined in (1.7) is real in coordinate space, the Lindblad contribution can be written in a simpler form by changing the transverse integration variable $\boldsymbol{p} \to -\boldsymbol{p}$ in the h.c term in (2.14):

$$\delta\langle\hat{O}\rangle_{|_L} = \frac{1}{2}\int_{E<p^-<Ee^\Delta} \frac{d^3p}{(2\pi)^3}\frac{1}{2p^+}\langle[C(-p),[\hat{O},C(p)]]\rangle_E = \Delta\frac{1}{8\pi}\int\frac{d^2\boldsymbol{p}}{(2\pi)^2}\langle[C(-p),[\hat{O},C(p)]]\rangle_{p^+=\boldsymbol{p}^2/2E} \tag{2.15}$$

Here we have taken the limit of infinitesimally small Δ, and will follow this practice without further comments in the following.

To calculate the commutator we use

$$[\rho^a(p^+,\boldsymbol{p}),\rho^b(q^+,\boldsymbol{q})] = if^{abc}\rho^c(max\{p^+,q^+\},\boldsymbol{p}+\boldsymbol{q}) = -T^c_{ab}\rho^c(max\{p^+,q^+\},\boldsymbol{p}+\boldsymbol{q}) \tag{2.16}$$

Now performing some simple algebra for $\hat{O}$ defined in (2.11) and calculating the double commutator we obtain

$$\begin{aligned}
&\delta\langle\rho^a(l^+,-\boldsymbol{q})\rho^a(m^+,\boldsymbol{q})\rangle_{|_L} = \Delta\frac{g^2N_c}{8\pi}\int\frac{d^2\boldsymbol{p}}{(2\pi)^2}\frac{4}{\boldsymbol{p}^2}\Big[\langle 2\rho^a(max\{p^+,l^+\},-\boldsymbol{q}+\boldsymbol{p})\rho^a(\max\{p^+,m^+\},-\boldsymbol{p}+\boldsymbol{q})\\
&-\rho^a(m^+,\boldsymbol{q})\rho^a(max\{p^+,l^+\},-\boldsymbol{q}) - \rho^a(\max\{p^+,m^+\},\boldsymbol{q})\rho^a(l^+,-\boldsymbol{q})\rangle_E\Big]_{p^+=\boldsymbol{p}^2/2E} = \Delta\frac{g^2N_c}{8\pi}\\
&\times\Bigg[\int_{\boldsymbol{p}^2<2Em^+}\frac{d^2\boldsymbol{p}}{(2\pi)^2}\frac{4}{\boldsymbol{p}^2}\langle 2\rho^a(l^+,-\boldsymbol{q}+\boldsymbol{p})\rho^a(m^+,-\boldsymbol{p}+\boldsymbol{q}) - \rho^a(m^+,\boldsymbol{q})\rho^a(l^+,-\boldsymbol{q}) - \rho^a(m^+,\boldsymbol{q})\rho^a(l^+,-\boldsymbol{q})\rangle_E\\
&+\int_{2Em^+<\boldsymbol{p}^2<2El^+}\frac{d^2\boldsymbol{p}}{(2\pi)^2}\frac{4}{\boldsymbol{p}^2}\langle 2\rho^a(l^+,-\boldsymbol{q}+\boldsymbol{p})\rho^a(p^+,-\boldsymbol{p}+\boldsymbol{q}) - \rho^a(m^+,\boldsymbol{q})\rho^a(l^+,-\boldsymbol{q}) - \rho^a(p^+,\boldsymbol{q})\rho^a(l^+,-\boldsymbol{q})\rangle_E\\
&+\int_{2El^+<\boldsymbol{p}^2}\frac{d^2\boldsymbol{p}}{(2\pi)^2}\frac{4}{\boldsymbol{p}^2}\langle 2\rho^a(p^+,\boldsymbol{q}-\boldsymbol{p})\rho^a(p^+,\boldsymbol{p}-\boldsymbol{q}) - \rho^a(m^+,\boldsymbol{q})\rho^a(p^+,-\boldsymbol{q}) - \rho^a(p^+,\boldsymbol{q})\rho^a(l^+,-\boldsymbol{q})\rangle\Bigg]_{p^+=\frac{\boldsymbol{p}^2}{2E}}
\end{aligned} \tag{2.17}$$

2.0.2 The Non-Lindblad term

We now proceed to calculate the terms in the evolution that involve directly the scattering of a gluon with frequency E emitted in the last step of the evolution. This contribution to the evolution is given by the following general expression (assuming $\langle 0|\hat{O}|0\rangle_F = 0$)

$$\delta\langle\hat{O}\rangle_{|_{NL}} = \int_{p,\bar{p}:p^-=\bar{p}^-=E}\langle C_i^{\dagger a}(p)\,\langle 0|A_i^a(p)\hat{O}A_j^{\dagger b}(\bar{p})|0\rangle_F\,C_j^b(\bar{p})\rangle_E \tag{2.18}$$

where the inner average is taken over the vacuum of the soft modes in the window and the outer in the state evolved to energy E. Here it is understood that at least one gluon annihilation operator in $\hat{O}$ acts on

the explicit $A^\dagger$ to the right of it, and at least one gluon creation operator acts on A to the left. Formally this can be written as

$$\delta\langle\hat{O}\rangle_{|_{NL}} = \int_{p,\bar{p}:p^-=\bar{p}^-=E} \langle C_i^{\dagger a}(p)\,\langle 0|[A_i^a(p),[\hat{O},A_j^{\dagger b}(\bar{p})]]|0\rangle_F\, C_j^b(\bar{p})\rangle_E \tag{2.19}$$

Let us first calculate the inner average in (2.19), i.e. average over the vacuum of the gluons in the window

$$\langle 0|[A_i^a(p),[\rho^c(l^+,-\boldsymbol{q})\rho^c(m^+,\boldsymbol{q}),A_j^{\dagger b}(\bar{p})]]|0\rangle_F = \frac{T^c_{ab}\delta_{ij}}{2\sqrt{p^+\bar{p}^+}}\Big\{\rho^c(l^+,-\boldsymbol{q})\delta^2(\boldsymbol{p}-\bar{\mathbf{p}}-\boldsymbol{q})\delta(p^+-\bar{p}^+)\theta(p^+-m^+)$$
$$+\rho^c(m^+,\boldsymbol{q})\delta^2(\boldsymbol{p}-\bar{\mathbf{p}}+\boldsymbol{q})\delta(p^+-\bar{p}^+)\theta(p-l^+)+\delta^2(\boldsymbol{p}-\bar{\mathbf{p}})\delta(\bar{p}^+-p^+)\theta(p^+-l^+)+...\Big\} \tag{2.20}$$

The first two term here correspond to the situation when one gluon from the window scatters via a single gluon exchange, while the second gluon that scatters is one of the pre-existing low frequency gluons. The last term describes the double scattering of one newly produced gluon. Two additional terms arise in contractions between the gluon operators in ρ and those in C and $C^\dagger$. However those terms do not vanish only if $(p\pm q)^-<E$, $(\bar{p}\pm q)^-<E$. In the limit $\Delta\to 0$ these terms are suppressed since they are proportional to Δ^2, and thus do not contribute to the derivative with respect to rapidity. We have denoted those terms by ellipsis in (2.20) and will neglect them in the following.

The first two terms can be brought into the form quadratic in the charge density operators. Consider the first term in (2.20) inserted into (2.19)

$$g^2\int_{p:p^-=(p-q)^-=E}\frac{1}{2p^+}\frac{\boldsymbol{p}\cdot(\boldsymbol{p}-\boldsymbol{q})}{\boldsymbol{p}^2(\boldsymbol{p}-\boldsymbol{q})^2}\langle\rho^a(p^+,\boldsymbol{p})\rho^c(l^+,-\boldsymbol{q})\rho^b(p^+,-\boldsymbol{p}+\boldsymbol{q})T^c_{ab}\theta(p^+-m^+)\rangle_E \tag{2.21}$$
$$=g^2\int_{p:p^-=(p-q)^-=E,p^+>m^+}\frac{1}{2p^+}\frac{\boldsymbol{p}\cdot(\boldsymbol{p}-\boldsymbol{q})}{\boldsymbol{p}^2(\boldsymbol{p}-\boldsymbol{q})^2}\langle\rho^c(l^+,-\boldsymbol{q})\rho^a(p^+,\boldsymbol{p})\rho^b(p^+,-\boldsymbol{p}+\boldsymbol{q})T^c_{ab}$$
$$-T^a_{cd}\rho^d(p^+,\boldsymbol{p}-\boldsymbol{q})\rho^b(p^+,-\boldsymbol{p}+\boldsymbol{q})T^c_{ab}\theta(p^+-l^+)-T^a_{cd}\rho^d(l^+,\boldsymbol{p}-\boldsymbol{q})\rho^b(p^+,-\boldsymbol{p}+\boldsymbol{q})T^c_{ab}\theta(l^+-p^+)\rangle_E$$
$$=g^2\int_{p:p^-=(p-q)^-=E,p^+>m^+}\frac{1}{2p^+}\frac{\boldsymbol{p}\cdot(\boldsymbol{p}-\boldsymbol{q})}{\boldsymbol{p}^2(\boldsymbol{p}-\boldsymbol{q})^2}\langle\frac{1}{2}\rho^c(l^+,-\boldsymbol{q})[\rho^a(p^+,\boldsymbol{p}),\rho^b(p^+,-\boldsymbol{p}+\boldsymbol{q})]T^c_{ab}$$
$$-N_c\rho^a(p^+,\boldsymbol{p}-\boldsymbol{q})\rho^a(p^+,-\boldsymbol{p}+\boldsymbol{q})\theta(p^+-l^+)-N_c\rho^a(l^+,\boldsymbol{p}-\boldsymbol{q})\rho^a(p^+,-\boldsymbol{p}+\boldsymbol{q})\theta(l^+-p^+)\rangle_E$$
$$=g^2\int_{p:p^-=(p-q)^-=E,p^+>m^+}\frac{1}{2p^+}\frac{\boldsymbol{p}\cdot(\boldsymbol{p}-\boldsymbol{q})}{\boldsymbol{p}^2(\boldsymbol{p}-\boldsymbol{q})^2}\langle\frac{N_c}{2}\rho^a(l^+,-\boldsymbol{q})\rho^a(p^+,\boldsymbol{q}))$$
$$-N_c\rho^a(p^+,\boldsymbol{p}-\boldsymbol{q})\rho^a(p^+,-\boldsymbol{p}+\boldsymbol{q})\theta(p^+-l^+)-N_c\rho^a(l^+,\boldsymbol{p}-\boldsymbol{q})\rho^a(p^+,-\boldsymbol{p}+\boldsymbol{q})\theta(l^+-p^+)\rangle_E$$

Here to get the first equality we have commuted the first two factors of ρ, while to get the second equality we have changed variables $\boldsymbol{p}\to-\boldsymbol{p}+\boldsymbol{q}$ in half of the terms (which is allowed since the frequencies of p and $p-q$ are equal) to obtain a commutator.

In the above, the vector $p-q$ is defined as $(p^+,\boldsymbol{p}-\boldsymbol{q})$ as is required by the delta function in (2.20). Thus the integration limit $p^-=(p-q)^-$ is equivalent to $\boldsymbol{p}^2=(\boldsymbol{p}-\boldsymbol{q})^2$. However the condition $\boldsymbol{p}^2=(\boldsymbol{p}-\boldsymbol{q})^2$ is very restrictive. For a fixed $\boldsymbol{q}$ it either does not allow any $\boldsymbol{p}$ at all (for $|\boldsymbol{p}|>|\boldsymbol{q}|$), or allows $\boldsymbol{p}$ with a fixed angle relative to the vector $\boldsymbol{q}$: $\cos\phi=\frac{\boldsymbol{q}^2}{2|\boldsymbol{p}||\boldsymbol{q}|}$ (for $|\boldsymbol{p}|<|\boldsymbol{q}|$). The entire contribution of (2.21) to the $\boldsymbol{p}$ integral is therefore measure zero and can be summarily dismissed.

A similar calculation for the second term in (2.20) leads to the same conclusion - this term is also measure zero in the $\boldsymbol{p}$ integral and we neglect it as well. Thus the only term that is of order Δ (as opposed

to Δ^2) in (2.20) is given by the last term. We then get

$$\delta\langle\rho^a(\boldsymbol{q})\rho^a(-\boldsymbol{q})\rangle_{|_{NL}} = \Delta\frac{g^2N_c}{\pi}\int_{\boldsymbol{p}^2\geq 2El^+}\frac{d^2\boldsymbol{p}}{(2\pi)^2}\frac{1}{\boldsymbol{p}^2}\left[\langle\rho^a(p^+,\boldsymbol{p})\rho^a(p^+,-\boldsymbol{p})\rangle_E\right]_{p^+=\frac{\boldsymbol{p}^2}{2E}} \tag{2.22}$$

2.0.3 The lopsided term

Finally we have to tackle the "lopsided" contribution. This contribution arises from the situation where only one of the wave functions in (2.13) is expanded to first order in C, whereas the other one is taken at oder zero:

$$\begin{aligned}\delta\langle\rho^a(m^+,\boldsymbol{q})\rho^a(l^+,-\boldsymbol{q})\rangle_{|_{LC}} &= \int_{p:E<p^-<Ee^\Delta}\frac{d^3p}{(2\pi)^3}\langle\rho^a(m^+,\boldsymbol{q})\rho^a(l^+,-\boldsymbol{q})A_i^{\dagger c}(p)C_i^c(p)+h.c.\rangle_E \\ &= \int_{p:E<p^-<Ee^\Delta}\frac{d^3p}{(2\pi)^3}\frac{g}{\sqrt{2p^+}}\frac{2i\boldsymbol{p}_i}{\boldsymbol{p}^2}\langle\Big[\rho^a(m^+,\boldsymbol{q})a_i^{\dagger b}(p^+,\boldsymbol{p}-\boldsymbol{q})\theta(p^+-l^+) \\ &\quad +a_i^{\dagger b}(p^+,\boldsymbol{p}+\boldsymbol{q})\rho^a(l^+,-\boldsymbol{q})\theta(p^+-m^+)\Big]T^a_{bc}\rho^c(p^+,-\boldsymbol{p})\rangle_E+h.c.\end{aligned} \tag{2.23}$$

The average in the equation above is over the LCWF at energy E, so that all the remaining creation and annihilation operators have to have frequency below E. To calculate the averages on the RHS of this equation we note that, since we expect that the gluon density in the wave function peaks close to the kinematic boundary of the highest frequency, the average is dominated by the configurations where the gluon created by the explicit $a^\dagger$ on the RHS has frequency close to E. If this is the case, the wave function for this gluon is perturbative, and to the leading order in α_s we can take it as the usual coherent state [40]. We then have,

$$\begin{aligned}&\delta\langle\rho^a(m^+,\boldsymbol{q})\rho^a(l^+,-\boldsymbol{q})\rangle_{|_{LC}} \\ &= -\int_{p:E<p^-<Ee^\Delta}\frac{d^3p}{(2\pi)^3}\frac{4g^2}{2p^+}\Big\langle T^a_{bc}\rho^c(p^+,-\boldsymbol{p})\Big[\frac{\boldsymbol{p}\cdot(\boldsymbol{p}-\boldsymbol{q})}{\boldsymbol{p}^2(\boldsymbol{p}-\boldsymbol{q})^2}\rho^b(p^+,\boldsymbol{p}-\boldsymbol{q})\rho^a(m^+,\boldsymbol{q})\theta(p^+-l^+) \\ &+\frac{\boldsymbol{p}\cdot(\boldsymbol{p}+\boldsymbol{q})}{\boldsymbol{p}^2(\boldsymbol{p}+\boldsymbol{q})^2}\rho^b(p^+,\boldsymbol{p}+\boldsymbol{q})\rho^a(l^+,-\boldsymbol{q})\theta(p^+-m^+)\Big]\Big\rangle_E+h.c. \\ &= -\int_{p:E<p^-<Ee^\Delta}\frac{d^3p}{(2\pi)^3}\frac{4g^2}{2p^+}\frac{\boldsymbol{p}\cdot(\boldsymbol{p}-\boldsymbol{q})}{\boldsymbol{p}^2(\boldsymbol{p}-\boldsymbol{q})^2}\Big[\langle\rho^b(p^+,\boldsymbol{p}-\boldsymbol{q})\rho^a(m^+,\boldsymbol{q})T^a_{bc}\rho^c(p^+,-\boldsymbol{p})\theta(p^+-l^+) \\ &+\rho^b(p^+,-\boldsymbol{p}+\boldsymbol{q})\rho^a(l^+,-\boldsymbol{q})T^a_{bc}\rho^c(p^+,\boldsymbol{p})\theta(p^+-m^+)\rangle_E\Big]\end{aligned} \tag{2.24}$$

Some terms on the RHS combine into commutators

$$\begin{aligned}&\delta\langle\rho^a(m^+,\boldsymbol{q})\rho^a(l^+,-\boldsymbol{q})\rangle_{|_{LC}} \\ &= -\int_{p:E<p^-<Ee^\Delta}\frac{d^3p}{(2\pi)^3}\frac{4g^2}{2p^+}\frac{\boldsymbol{p}\cdot(\boldsymbol{p}-\boldsymbol{q})}{\boldsymbol{p}^2(\boldsymbol{p}-\boldsymbol{q})^2}\Big[\Big\{[\langle\rho^b(p^+,\boldsymbol{p}-\boldsymbol{q}),\rho^a(m^+,\boldsymbol{q})]T^a_{bc}\rho^c(p^+,-\boldsymbol{p}) \\ &-T^d_{ca}\rho^d(p^+,-\boldsymbol{p}+\boldsymbol{q})\rho^a(p^+,\boldsymbol{p}-\boldsymbol{q})T^a_{bc}-T^d_{cb}\rho^a(m^+,\boldsymbol{q})\rho^d(p^+,-\boldsymbol{q})T^a_{bc}\rangle_E\Big\}\theta(p^+-l^+) \\ &+(\boldsymbol{p},\boldsymbol{q},l^+)\to(-\boldsymbol{p},-\boldsymbol{q},m^+)\Big]\end{aligned} \tag{2.25}$$

After some algebra,

$$\begin{aligned}
&\delta\langle\rho^a(m^+,\boldsymbol{q})\rho^a(l^+,-\boldsymbol{q})\rangle_{|LC}\\
&\quad=-\int_{p:E<p^-<Ee^\Delta}\frac{d^3p}{(2\pi)^3}\frac{4g^2N_c}{2p^+}\frac{\boldsymbol{p}\cdot(\boldsymbol{p}-\boldsymbol{q})}{\boldsymbol{p}^2(\boldsymbol{p}-\boldsymbol{q})^2}\Big[\langle\Big\{\rho^a(p^+,\boldsymbol{p})\rho^a(p^+,-\boldsymbol{p})+\rho^a(p^+,-\boldsymbol{p}+\boldsymbol{q})\rho^a(p^+,\boldsymbol{p}-\boldsymbol{q})\\
&\quad-\rho^a(m^+,\boldsymbol{q})\rho^a(p^+,-\boldsymbol{q})\Big\}\theta(p^+-l^+)\\
&\quad+\Big\{\rho^a(p^+,\boldsymbol{p})\rho^a(\max\{p^+,l^+\},-\boldsymbol{p})+\rho^a(p^+,-\boldsymbol{p}+\boldsymbol{q})\rho^a(\max\{p^+,l^+\},\boldsymbol{p}-\boldsymbol{q})\\
&\quad-\rho^a(l^+,-\boldsymbol{q})\rho^a(p^+,\boldsymbol{q})\Big\}\theta(p^+-m^+)\rangle_E\Big]
\end{aligned}\tag{2.26}$$

Finally, we obtain

$$\begin{aligned}
&\delta\langle\rho^a(m^+,\boldsymbol{q})\rho^a(l^+,-\boldsymbol{q})\rangle_{|LC}\\
&\quad=-\Delta\frac{2g^2N_c}{\pi}\int_{\boldsymbol{p}^2\geq 2El^+}\frac{d^2\boldsymbol{p}}{(2\pi)^2}\frac{\boldsymbol{p}\cdot(\boldsymbol{p}-\boldsymbol{q})}{\boldsymbol{p}^2(\boldsymbol{p}-\boldsymbol{q})^2}\langle\rho^a(p^+,\boldsymbol{p})\rho^a(p^+,-\boldsymbol{p})+\rho^a(p^+,-\boldsymbol{p}+\boldsymbol{q})\rho^a(p^+,\boldsymbol{p}-\boldsymbol{q})\\
&\qquad-\frac{1}{2}\Big(\rho^a(m^+,\boldsymbol{q})\rho^a(p^+,-\boldsymbol{q})+\rho^a(l^+,-\boldsymbol{q})\rho^a(p^+,\boldsymbol{q})\Big)\rangle_{p^+=\frac{\boldsymbol{p}^2}{2E}}\\
&\qquad-\Delta\frac{g^2N_c}{\pi}\int_{2Em^+\leq\boldsymbol{p}^2\leq 2El^+}\frac{d^2\boldsymbol{p}}{(2\pi)^2}\frac{\boldsymbol{p}\cdot(\boldsymbol{p}-\boldsymbol{q})}{\boldsymbol{p}^2(\boldsymbol{p}-\boldsymbol{q})^2}\langle\rho^a(p^+,\boldsymbol{p})\rho^a(l^+,-\boldsymbol{p})+\rho^a(p^+,-\boldsymbol{p}+\boldsymbol{q})\rho^a(l^+,\boldsymbol{p}-\boldsymbol{q})\\
&\qquad-\rho^a(l^+,-\boldsymbol{q})\rho^a(p^+,\boldsymbol{q})\rangle_{p^+=\frac{\boldsymbol{p}^2}{2E}}
\end{aligned}\tag{2.27}$$

2.0.4 The BO-BFKL equation

We now collect all the information. Combining all the contributions (L+NL+LC) and dividing by Δ we obtain a differential evolution:

$$\frac{\partial\langle\hat{O}\rangle}{\partial\eta}=\lim_{\Delta\to 0}\frac{\delta\langle\hat{O}\rangle}{\Delta}\,;\qquad\qquad\eta\equiv\ln E/E_0.\tag{2.28}$$

For the ρ correlator this reads

$$\begin{aligned}
&\frac{\partial}{\partial\eta}\langle\rho^a(m^+,\boldsymbol{q})\rho^a(l^+,-\boldsymbol{q})\rangle=\frac{g^2N_c}{\pi}\\
&\times\int_{\boldsymbol{p}^2\geq 2El^+}\left[\frac{1}{\boldsymbol{p}^2}-\left\{\frac{2\boldsymbol{p}\cdot(\boldsymbol{p}-\boldsymbol{q})}{\boldsymbol{p}^2(\boldsymbol{p}-\boldsymbol{q})^2}\right\}_{\boldsymbol{p}^2\geq(\boldsymbol{p}-\boldsymbol{q})^2}\right]\\
&\times\Big\langle\left\{\rho^a(p^+,\boldsymbol{p})\rho^a(p^+,-\boldsymbol{p})+\rho^a(p^+,\boldsymbol{q}-\boldsymbol{p})\rho^a(p^+,\boldsymbol{p}-\boldsymbol{q})-\frac{1}{2}\Big[\rho^a(m^+,\boldsymbol{q})\rho^a(p^+,-\boldsymbol{q})+\rho^a(p^+,\boldsymbol{q})\rho^a(l^+,-\boldsymbol{q})\Big]\right\}\\
&+\int_{2Em^+\leq\boldsymbol{p}^2\leq 2El^+}\left\{\frac{1}{\boldsymbol{p}^2}\left\{\rho^a(l^+,-\boldsymbol{q}+\boldsymbol{p})\rho^a(p^+,-\boldsymbol{p}+\boldsymbol{q})-\frac{1}{2}\left[\rho^a(m^+,\boldsymbol{q})\rho^a(l^+,-\boldsymbol{q})+\rho^a(p^+,\boldsymbol{q})\rho^a(l^+,-\boldsymbol{q})\right]\right\}\right.\\
&\left.-\left\{\frac{\boldsymbol{p}\cdot(\boldsymbol{p}-\boldsymbol{q})}{\boldsymbol{p}^2(\boldsymbol{p}-\boldsymbol{q})^2}\right\}_{\boldsymbol{p}^2\geq(\boldsymbol{p}-\boldsymbol{q})^2}\left[\rho^a(p^+,\boldsymbol{p})\rho^a(l^+,-\boldsymbol{p})+\rho^a(p^+,-\boldsymbol{p}+\boldsymbol{q})\rho^a(l^+,\boldsymbol{p}-\boldsymbol{q})-\rho^a(l^+,-\boldsymbol{q})\rho^a(p^+,\boldsymbol{q})\right]\right\}\\
&+\int_{\boldsymbol{p}^2<2Em^+}\frac{d^2\boldsymbol{p}}{(2\pi)^2}\frac{1}{\boldsymbol{p}^2}\Big\{\rho^a(l^+,-\boldsymbol{q}+\boldsymbol{p})\rho^a(m^+,-\boldsymbol{p}+\boldsymbol{q})-\rho^a(m^+,\boldsymbol{q})\rho^a(l^+,-\boldsymbol{q})\Big\}\Big\rangle
\end{aligned}\tag{2.29}$$

where the longitudinal momentum p^+ is given by $p^+=\frac{\boldsymbol{p}^2}{2E}$.

We note that this equation is very reminiscent to the standard BFKL equation. Suppose we can neglect the p^+ dependence in the correlators and also take $l^+ = m^+ = 0$, which is what one routinely does in the BFKL framework. We are then left only with the first and third lines. Moreover, the third line is the complement of the first line with the integration region $\boldsymbol{p}^2 \leq (\boldsymbol{p}-\boldsymbol{q})^2$, so that the total integration region of $\boldsymbol{p}^2$ integral is now unrestricted. We then change variables $\boldsymbol{p} \to -\boldsymbol{p} + \boldsymbol{q}$ in the term involving $\rho(\boldsymbol{p}-\boldsymbol{q})$. Noting that

$$\frac{1}{(\boldsymbol{p}-\boldsymbol{q})^2} + \frac{1}{\boldsymbol{p}^2} - \frac{2\boldsymbol{p}\cdot(\boldsymbol{p}-\boldsymbol{q})}{\boldsymbol{p}^2(\boldsymbol{p}-\boldsymbol{q})^2} = \frac{\boldsymbol{q}^2}{\boldsymbol{p}^2(\boldsymbol{p}-\boldsymbol{q})^2} \ , \tag{2.30}$$

the equation becomes

$$\frac{\partial}{\partial\eta}\langle\rho^a(\boldsymbol{q})\rho^a(-\boldsymbol{q})\rangle = \frac{g^2N_c}{\pi}\int\frac{d^2\boldsymbol{p}}{(2\pi)^2}\frac{\boldsymbol{q}^2}{\boldsymbol{p}^2(\boldsymbol{p}-\boldsymbol{q})^2}\,\langle\rho^a(\boldsymbol{p})\rho^a(-\boldsymbol{p}) - \frac{1}{2}\rho^a(\boldsymbol{q})\rho^a(-\boldsymbol{q})\rangle \tag{2.31}$$

which is precisely the standard BFKL equation.

We have derived (2.29) taking the frequency of the production vertices $\boldsymbol{q}^2/2l^+$ and $\boldsymbol{q}^2/2m^+$ to be arbitrary. For the purpose of calculating the S matrix however we are interested in the frequency of order of the frequency of the target $q^- \sim E$. Taking the frequency in both color charge densities to be equal to E means we should take $l^+ = m^+ = \frac{\boldsymbol{q}^2}{2E} = \bar{q}^+$. Specifying to these values we obtain

$$\begin{aligned}
&\frac{\partial}{\partial\eta}\langle\rho^a(\bar{q}^+,\boldsymbol{q})\rho^a(\bar{q}^+,-\boldsymbol{q})\rangle = \frac{g^2N_c}{\pi}\int_{\boldsymbol{p}^2\geq\boldsymbol{q}^2}\left[\frac{1}{\boldsymbol{p}^2} - \left\{\frac{2\boldsymbol{p}\cdot(\boldsymbol{p}-\boldsymbol{q})}{\boldsymbol{p}^2(\boldsymbol{p}-\boldsymbol{q})^2}\right\}_{\boldsymbol{p}^2\geq(\boldsymbol{p}-\boldsymbol{q})^2}\right] \\
&\times\langle\rho^a(p^+,\boldsymbol{p})\rho^a(p^+,-\boldsymbol{p}) + \rho^a(p^+,\boldsymbol{q}-\boldsymbol{p})\rho^a(p^+,\boldsymbol{p}-\boldsymbol{q}) - \rho^a(\bar{q}^+,\boldsymbol{q})\rho^a(p^+,-\boldsymbol{q})\rangle \\
&+\int_{\boldsymbol{p}^2<\boldsymbol{q}^2}\frac{d^2\boldsymbol{p}}{(2\pi)^2}\frac{1}{\boldsymbol{p}^2}\langle\rho^a(\bar{q}^+,-\boldsymbol{q}+\boldsymbol{p})\rho^a(\bar{q}^+,-\boldsymbol{p}+\boldsymbol{q}) - \rho^a(\bar{q}^+,\boldsymbol{q})\rho^a(\bar{q}^+,-\boldsymbol{q})\rangle
\end{aligned} \tag{2.32}$$

where $\bar{q}^+ = \boldsymbol{q}^2/2E$ and $p^+ = \boldsymbol{p}^2/2E$. We will refer to (2.32) as the BO-BFKL equation, and are going to study it in the next section.

3 The intercept, the anomalous dimension and all that

Our goal now is to understand the properties of solutions of (2.32).

At first glance it looks like this equation is not closed, as its RHS contains terms nondiagonal in the longitudinal momentum. However the surprisingly simplifying property of this equation is that the integration boundaries over the transverse momentum do not involve the longitudinal momenta at all. This has an immediate consequence that (2.32) has solutions that do not depend on p^+. Moreover, for functions that do not depend on p^+, (2.32) is dilatationally invariant since it does not contain any transverse scale. This, in turn implies that the eigenfunctions of this equations are pure powers of transverse momentum, just like in the BFKL case. The equation is also rotationally invariant, which means that the eigenfunctions are characterized by the values of angular momentum, but in this paper we will study only rotationally invariant solutions.

Our focus is therefore on the eigenfunctions of the form

$$f_\gamma(\boldsymbol{p}) = \left[\frac{|\boldsymbol{p}|}{|\boldsymbol{p}_0|}\right]^\gamma \tag{3.1}$$

with $|\boldsymbol{p}_0|$ - an arbitrary scale. The evolution equation for the function f_γ is simply

$$\frac{\partial}{\partial\eta}f_\gamma(\boldsymbol{p}) = \frac{\bar\alpha_s}{\pi}\chi(\gamma)f_\gamma(\boldsymbol{p}) \tag{3.2}$$

where $\frac{\bar\alpha_s}{\pi}\chi(\gamma)$ is the eigenvalue of the operator on the RHS of (2.32), or the characteristic function, with $\bar\alpha_s \equiv \frac{\alpha_s N_c}{\pi}$.

We will next analyze the spectrum of eigenvalues $\chi(\gamma)$. Before embarking on this analysis we find it convenient to rewrite the equation in the form which makes it explicit that the UV properties of the kernel of RHS of (2.32) are the same as that of the BFKL. To do this we note that

$$\begin{aligned}
&\int_{\boldsymbol{p}^2>\boldsymbol{q}^2} d^2\boldsymbol{p}\ \ \frac{1}{\boldsymbol{p}^2}\Big[1-2\frac{(\boldsymbol{p}-\boldsymbol{q})\cdot\boldsymbol{p}}{(\boldsymbol{p}-\boldsymbol{q})^2}\Theta(\boldsymbol{p}^2-(\boldsymbol{p}-\boldsymbol{q})^2)\Big]\Big(f_\gamma(\boldsymbol{p})+f_\gamma(\boldsymbol{p}-\boldsymbol{q})\Big)\\
=&\int_{\boldsymbol{p}^2>\boldsymbol{q}^2} d^2\boldsymbol{p}\ \ \frac{1}{\boldsymbol{p}^2}\Big[1-2\frac{(\boldsymbol{p}-\boldsymbol{q})\cdot\boldsymbol{p}}{(\boldsymbol{p}-\boldsymbol{q})^2}\Theta(\boldsymbol{p}^2-(\boldsymbol{p}-\boldsymbol{q})^2)\Big]f_\gamma(\boldsymbol{p})\\
+&\int_{(\boldsymbol{p}-\boldsymbol{q})^2>\boldsymbol{q}^2} d^2\boldsymbol{p}\ \ \frac{1}{(\boldsymbol{p}-\boldsymbol{q})^2}\Big[1-2\frac{(\boldsymbol{p}-\boldsymbol{q})\cdot\boldsymbol{p}}{(\boldsymbol{p}-\boldsymbol{q})^2}\Theta((\boldsymbol{p}-\boldsymbol{q})^2-\boldsymbol{p}^2)\Big]f_\gamma(\boldsymbol{p})
\end{aligned} \tag{3.3}$$

where in the second term we shifted variables $\boldsymbol{p}\to\boldsymbol{q}-\boldsymbol{p}$. Thus for the common range of the two integrals, $|\boldsymbol{p}|>2|\boldsymbol{q}|$ the two θ-functions add up to unity. The UV part of the integral over $\boldsymbol{p}$ is therefore the same as in the BFKL equation. Using this change of variables we can write our eigenvalue equation as

$$\begin{aligned}
&\int_{\boldsymbol{p}^2>4\boldsymbol{q}^2} d^2\boldsymbol{p}\ \ \frac{\boldsymbol{q}^2}{\boldsymbol{p}^2(\boldsymbol{p}-\boldsymbol{q})^2}[f_\gamma(\boldsymbol{p})-\frac{1}{2}f_\gamma(\boldsymbol{q})]\\
+&\int_{(\boldsymbol{p}-\boldsymbol{q})^2>\boldsymbol{q}^2;\boldsymbol{p}^2<4\boldsymbol{q}^2} d^2\boldsymbol{p}\ \ \frac{1}{(\boldsymbol{p}-\boldsymbol{q})^2}\Big[1-2\frac{(\boldsymbol{p}-\boldsymbol{q})\cdot\boldsymbol{p}}{(\boldsymbol{p}-\boldsymbol{q})^2}\Theta((\boldsymbol{p}-\boldsymbol{q})^2-\boldsymbol{p}^2)\Big][f_\gamma(\boldsymbol{p})-\frac{1}{2}f_\gamma(\boldsymbol{q})]\\
+&\int_{\boldsymbol{q}^2<\boldsymbol{p}^2<4\boldsymbol{q}^2} d^2\boldsymbol{p}\ \ \frac{1}{\boldsymbol{p}^2}\Big[1-2\frac{(\boldsymbol{p}-\boldsymbol{q})\cdot\boldsymbol{p}}{(\boldsymbol{p}-\boldsymbol{q})^2}\Theta(\boldsymbol{p}^2-(\boldsymbol{p}-\boldsymbol{q})^2)\Big][f_\gamma(\boldsymbol{p})-\frac{1}{2}f_\gamma(\boldsymbol{q})]\\
+&\int_{\boldsymbol{p}^2<\boldsymbol{q}^2} d^2\boldsymbol{p}\frac{1}{\boldsymbol{p}^2}\Big(f_\gamma(\boldsymbol{p}+\boldsymbol{q})-f_\gamma(\boldsymbol{q})\Big)=\chi(\gamma)f_\gamma(\boldsymbol{q})
\end{aligned} \tag{3.4}$$

This equation has several interesting features. First of all, it is obvious that the UV behavior of the kernel is the same as those of the BFKL. We therefore are assured, that just like the BFKL, the eigenvalue diverges for $\gamma\geq 2$. Second, in contradistinction to the BFKL there is no IR divergence in the integral at $\boldsymbol{p}=0$ for any function $f_\gamma(\boldsymbol{p})$ which diverges at zero slower that $1/\boldsymbol{p}^2$, or $\gamma>-2$, due to the cancellation in the last term. Recall that for the BFKL equation the IR divergence appears already for $\gamma\leq 0$. This means that the divergence of the BFKL eigenvalue at $\gamma=0$ is not present and the eigenvalue $\chi(0)$ is finite.

The physical reason is easy to understand. For $\boldsymbol{p}^2\ll\boldsymbol{q}^2$ one would need to have $p^+\ll\bar q^+$ in order that the frequencies of the two momenta be the same. However particles with such small longitudinal momenta do not scatter eikonally on the target, and therefore do not contribute to the evolution of the cross section, even though they may be emitted in the wave function. Instead the IR divergence arises at $\gamma=-2$ due to $f_\gamma(\boldsymbol{p})$ in the second line and $f_\gamma(\boldsymbol{p}+\boldsymbol{q})$ in the last line since $f_{-2}(\boldsymbol{p})=1/\boldsymbol{p}^2$ is not integrable at zero (in the last line the singularity is at $\boldsymbol{p}=\boldsymbol{q}$). We therefore expect that the range of real eigenvalues for this equation is $-2<\gamma<2$.

We studied this equation numerically. The details of the numerical procedure are explained in Appendix A. In Fig.1 we present the numerical result for the characteristic function $\chi(\gamma)$ for real γ and compare it to the characteristic function of the BFKL equation. Fig.1 exhibits clearly all the features noted above.

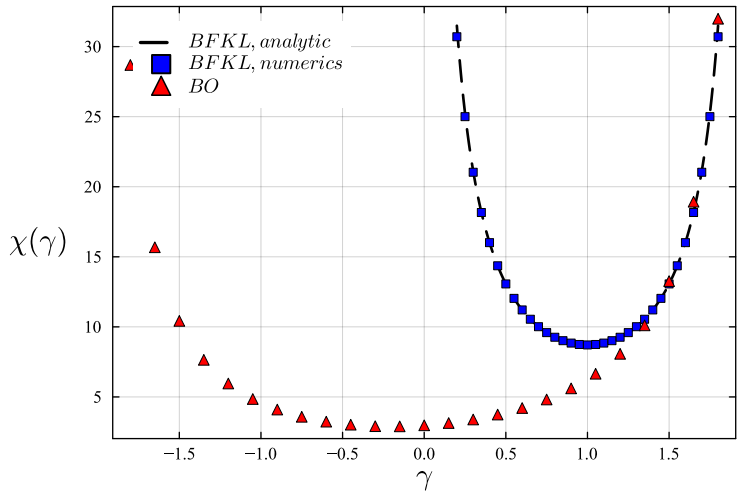

Figure 1: The charcteristic function of the BO-BFKL equation vs that of the BFKL as a function of real γ. The analytic expression for BFKL eigenvalue is $\chi_{BFKL}(\gamma) = \pi\Big[2\psi(1) - \psi(1-\frac{\gamma}{2}) - \psi(\frac{\gamma}{2})\Big]$, with the digamma function defined as $\psi(z) = \frac{d}{dz}\Gamma(z)$.

In addition to the real eigenvalues, the equation has of course also eigenvalues with complex γ. We will study those in the next subsection.

3.1 The scattering amplitude and the saddle point approximation

Since the eigenfunctions of (3.4) are the same as those of the BFKL equation, the expansion of the scattering amplitude at initial energy in our case is also the same. One needs to expand the scattering amplitude in the set of eigenfunctions f_γ with $\gamma = 1 + i\nu$ [41], since this set comprises a complete and orthonormal set of eigenfunctions. The scattering amplitude T at the start of the evolution at $E = E_0$ is therefore written as

$$T_{\eta=0}(\boldsymbol{p}) = \int_\nu C_\nu \left[\frac{|\boldsymbol{p}|}{|\boldsymbol{p}_0|}\right]^{\gamma-2} \tag{3.5}$$

where we have introduced an arbitrary scale $|\boldsymbol{p}_0|$ to make the dimensions of the coefficients C_ν the same. The extra factor $1/(\boldsymbol{p})^2$ is due to the fact that $T(\boldsymbol{q}) \sim \frac{1}{\boldsymbol{p}^2}\langle\rho(\boldsymbol{p})\rho(-\boldsymbol{p})\rangle$ (see (1.1)).

For a simple initial condition where the scattering occurs with a fixed momentum transfer $\boldsymbol{p}_0$, the scattering amplitude (up to overall normalization) is $\langle\rho(\boldsymbol{p})\rho(-\boldsymbol{p})\rangle = \delta^2(\boldsymbol{p} - \boldsymbol{p}_0)$, and the coefficients of the expansion are determined simply as [41]

$$C_\nu = 1\,. \tag{3.6}$$

At finite rapidity η the scattering amplitude then is

$$T_\eta(\boldsymbol{p}) = \int_\nu e^{\frac{\bar{\alpha}_s}{\pi}\chi(1+i\nu)\eta} e^{(-1+i\nu)\bar{\rho}} \tag{3.7}$$

with $\bar{\rho} \equiv \ln \frac{|\boldsymbol{p}|}{|\boldsymbol{p}_0|}$.

The integral in (3.7) is along the imaginary direction in the complex γ plane at the point $\Re(\gamma) = 1$. The first interesting question is what is the asymptotic behavior of the amplitude at very large η.

To determine the asymptotic behavior one can disregard the $\bar{\rho}$-dependent factor in (3.7), and study the simplified expression

$$t_\eta = \int_\nu e^{\frac{\bar{\alpha}_s}{\pi}\chi(1+i\nu)\eta} \tag{3.8}$$

For the BFKL spectrum $\chi_{BFKL}(\gamma)$ the integral over ν is dominated by the saddle point of the integral at $\nu = 0$ and therefore the asymptotic behavior is dominated by the eigenvalue $\chi_{BFKL}(0) = 4\pi \ln 2$.

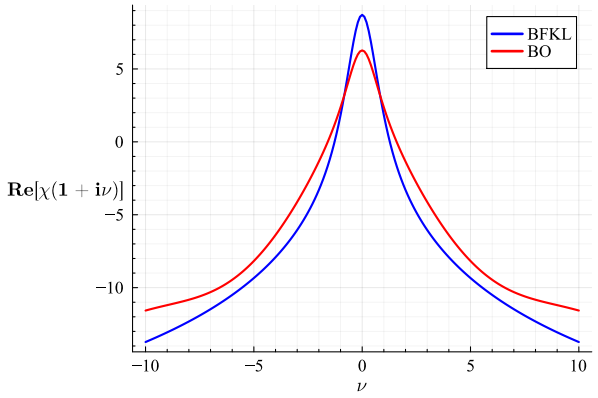

Figure 2: The real part of the BO-BFKL vs the BFKL characteristic functions as a function of ν for $\gamma = 1 + i\nu$.

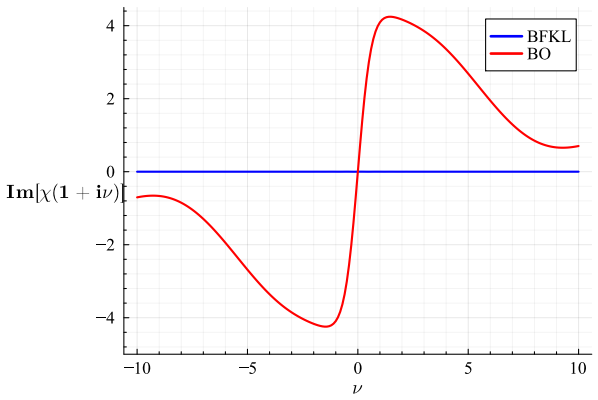

Figure 3: The imaginary part of the characteristic function for the BO-BFKL vs BFKL as a function of ν for $\gamma = 1 + i\nu$.

For the BO-BFKL this is clearly not the case. We plot the real and imaginary parts of $\chi(1 + i\nu)$ as a function of ν on Fig. 2 and Fig. 3. It is obvious that the point $\nu = 0$ is not a saddle point. This is not particularly surprising, given that the point $\gamma = 1$ is not a minimum of $\chi(\gamma)$ for real values of γ. If $\chi(\gamma)$ is an analytic function, for the saddle point to lie on the real axis, the function of course has to have a minimum along the real axis at this point. For the BFKL equation $\chi_{BFKL}(\gamma)$ is an analytic function and indeed $\chi_{BFKL}(1)$ is a minimum and therefore the saddle point lies on the real axis and also directly on the integration contour in the complex plane. For the BO-BFKL, since we do not have the analytic form

of $\chi(\gamma)$, we do not know whether it is an analytic function. If it were, we would expect the saddle point to appear at $\Re(\gamma) = -0.2$.

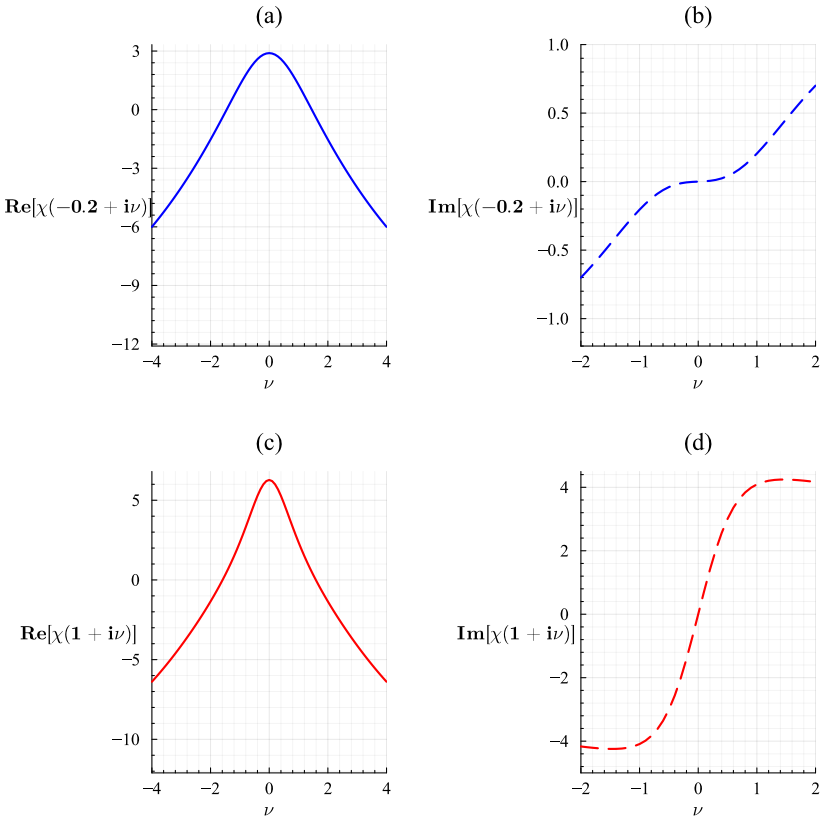

Figure 4: Comparison of the real and imaginary parts of the BO-BFKL characteristic function $\chi(\gamma)$ for $\Re(\gamma) = 1$ and $\Re(\gamma) = -0.2$.

Indeed plotting the function $\chi(-0.2 + i\nu)$ (see Fig. 4) we observe that the first derivative with respect to ν vanishes at $\nu = 0$. It therefore looks very likely that the saddle point of the integral in the complex plane is at $\gamma = -0.2$. The plot of the imaginary part of $\chi(\gamma)$ on Fig. 4 confirms the existence of the saddle point. On Fig. 5 we plot $\chi(\gamma)$ as a function of complex γ and indeed observe this behavior.

All this makes us believe that in order to calculate the integral (3.8) we may deform the integration contour in the complex γ plane so that it goes through the saddle point at $\gamma = -0.2$ and calculate the integral in the steepest descent approximation. Strictly speaking we do not know if this is allowed, as we do not have a mathematical proof that the function $\chi(\gamma)$ is analytic. We therefore study this question numerically. On Fig. 7 we plot the logarithm of the integral (3.8) calculated along the straight line $\gamma = 1$ versus the same integral calculated along the straight line $\gamma = -0.2$ which passes through the saddle point. For very high values of rapidity our numerics becomes unstable, but for all values of η where the numerics is stable the two integrals give identical results. The integral at $\gamma = -0.2$ can be calculated in the saddle point approximation. On Fig. 8 we compare the result of the numerical integration with the result of the saddle point approximation for large range of rapidities. The two are indeed very close.

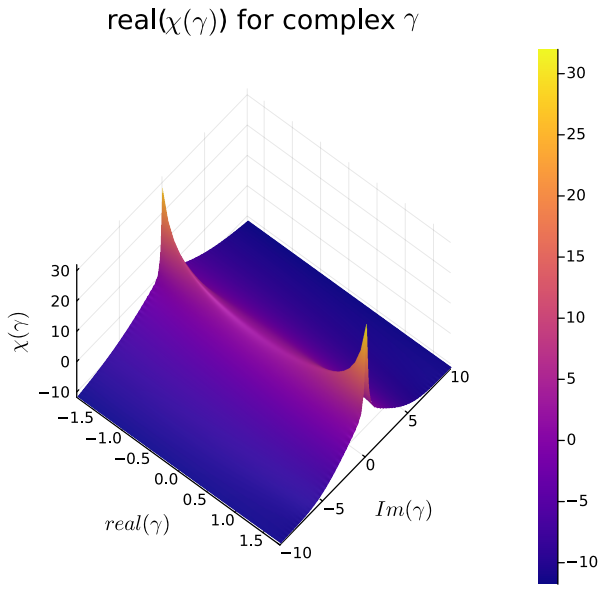

Figure 5: 3D plot of Re$[\chi(\gamma)]$.

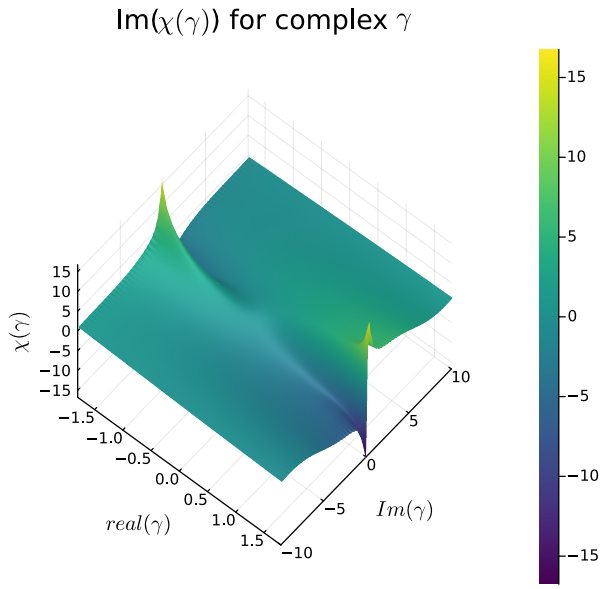

Figure 6: 3D plot of Im$[\chi(\gamma)]$.

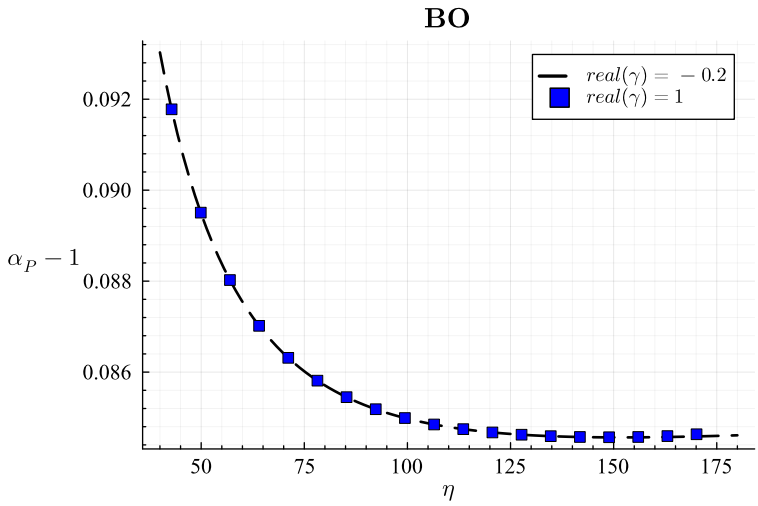

Figure 7: The logarithm of the integral in (3.8) calculated along the line $\gamma = 1$ and $\gamma = -0.2$ as a function of rapidity: $\alpha_P - 1 \equiv \frac{\ln t_\eta}{\eta}$ for $\alpha_s = 0.1$.

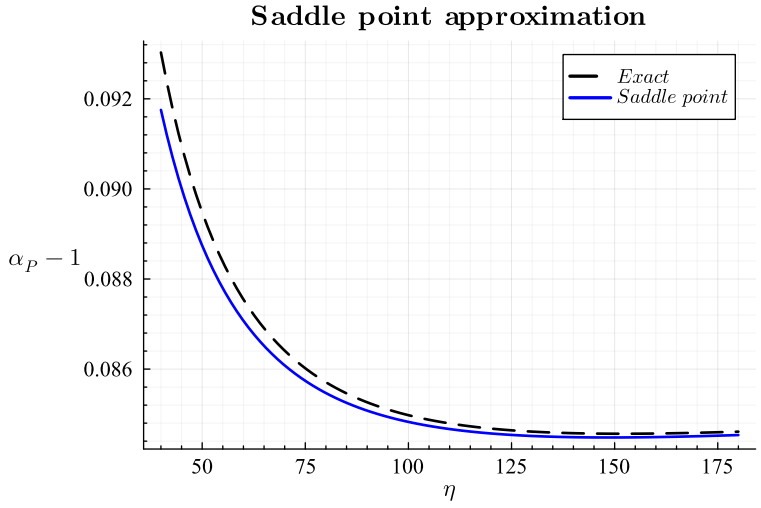

Figure 8: Exact numerical evaluation vs the steepest descent result for the "Pomeron intercept" defined as $\alpha_P - 1 \equiv \frac{\ln t_\eta}{\eta}$ for $\alpha_s = 0.1$. Note that α_P changes very little in the above wide range of rapidities with the bulk of the change explained by the variation of the pre exponential factor in (3.9).

3.2 The Pomeron intercept and the anomalous dimension

In the saddle point approximation the analytic result for the integral (3.8) is

$$t_\eta = \pi \sqrt{\frac{1}{1.89 \bar{\alpha}_s}} \eta^{-1/2} e^{\bar{\alpha}_s 0.91 \eta} \tag{3.9}$$

Here we have determined numerically $\chi(\gamma_0^{BO} = -0.2) = 2.89$ and $\frac{1}{2}\Re\left[\frac{d^2\chi(-0.2+i\nu)}{d\nu^2}\right]_{\nu=0} = -1.89$.

Comparing the value of the constant in the exponent, 0.91 with the BFKL value $4 \ln 2 \approx 2.77$ we observe that the Pomeron intercept in the BO-BFKL calculation is dramatically lower - by about a factor of three - than in the standard BFKL.

For asymptotically large η the saddle point in the integral (3.7) is the same as in (3.8). Thus the leading momentum dependence of the scattering amplitude is given by

$$T_\eta(\boldsymbol{k}) \sim \frac{1}{\boldsymbol{k}^2} |\boldsymbol{k}|^{-0.2} \tag{3.10}$$

We again find a very significant difference with the BFKL equation. The anomalous dimension in the asymptotic regime for the BO-BFKL is $\gamma_0^{BO} = -0.2$ rather than the BFKL value of 1.

3.3 The saturation boundary and saturation momentum

Another interesting quantity to study is the properties of saturation inherent in our equation. Although complete study of the saturation dynamics requires extension of our present calculation to include multiple scattering effects, and this is beyond present work, we can get a rough idea by using the simple proxy method devised in [39]. In order to infer the dependence of saturation momentum on rapidity, [39] imposed the saturation boundary on the BFKL evolution, and this method can be applied to the BO-BFKL evolution

as well. The most primitive variant of the calculation that we use here is to study a saddle point of the amplitude (3.7) for transverse momenta such that the exponential growth of the amplitude with rapidity is offset by the momentum dependence of the eigenfunction. The saturation momentum then is identified with the value of momentum at which the exponential factor is of order unity. This approach yields two equations

$$\frac{\bar{\alpha}_s}{\pi}\chi'(\gamma)\eta + \bar{\rho} = 0; \qquad \frac{\bar{\alpha}_s}{\pi}\chi(\gamma) + (\gamma - 2)\bar{\rho} = 0\,. \tag{3.11}$$

The first one is the saddle point equation which does not neglect the existence of the factor $e^{(-2+\gamma)\bar{\rho}}$ in (3.7), while the second is the requirement that the value of the scattering amplitude is of order unity.

The resulting equation for the position of the saturation saddle point is [39]

$$\chi'(\gamma) = \frac{\chi(\gamma)}{\gamma - 2} \tag{3.12}$$

Solving numerically this equation we find,

$$\gamma_s = -0.487\,; \qquad \chi(\gamma_s) = 3.063 \tag{3.13}$$

The value of the saturation momentum as a function of rapidity is given by (3.11) as

$$Q_s^2 = \boldsymbol{p}_0^2 \exp\{\frac{2}{\pi}\frac{\chi(\gamma_s)}{2-\gamma_s}\bar{\alpha}_s\eta\} = \boldsymbol{p}_0^2 \exp\{0.784\bar{\alpha}_s\eta\} \tag{3.14}$$

We note that for the BFKL calculation the analogous result is [39]

$$Q_{BFKL}^2 = \boldsymbol{p}_0^2 \exp\{4.88\bar{\alpha}_s\eta\} \tag{3.15}$$

The two expressions are even more strikingly different that the asymptotics of the scattering amplitude, as the ratio between the factors in the exponent is now about six rather than three. The reason is that the BO-BFKL characteristic function is rather flat in the vicinity of the saddle point, and thus the value of $\chi(\gamma)$ at the saturation saddle point is not very different than at the minimum. For the BFKL on the other hand the characteristic function varies mush faster, which leads to a more significant difference between the values of χ at the two saddle points.

4 Conclusions

In this paper we applied the Born-Oppenheimer renormalization group approach to eikonal scattering. We have approximated both the scattering amplitude and the evolution kernel by the appropriate eikonal expressions in the whole kinematically available range. One crucial difference of our approach vs the standard BFKL calculation is that we explicitly keep the longitudinal momentum dependence of the emission amplitude. As a result, even though the formulae are eikonal, they preserve the momentum conservation in the sense that the longitudinal momentum of the emitted particle is always limited from above by the momentum of the emitter.

We have derived a linear evolution equation, the BO-BFKL equation for the scattering amplitude which shares many common properties with the BFKL equation. It is dilatationally and rotationally (although not conformally) invariant. Moreover, the eigenfunctions of the BO-BFKL equation do not depend on the

longitudinal momentum. As a result these eigenfunctions are the same as those of the standard BFKL equation - pure powers of the transverse momentum: $f_\gamma(\boldsymbol{p}) \sim |\boldsymbol{p}|^\gamma$.

The UV properties of the BO-BFKL kernel are identical with those of the standard BFKL kernel. However the IR properties of the two kernels are markedly different: the BO-BFKL kernel is notably softer. Physically we understand this property as a direct consequence of momentum conservation coupled with the frequency ordering in the BO approach: although gluons with very low transverse momentum are emitted during the evolution, frequency ordering requires that their longitudinal momentum be so small that they cannot participate in eikonal scattering and therefore do not contribute to the evolution of the amplitude.

This difference in the infrared leads to striking difference between the resulting scattering amplitudes. We studied numerically the characteristic function of the BO-BFKL equation, $\chi(\gamma)$. The first major difference is that the range of the allowed eigenvalues for the BO-BFKL is $-2 < \gamma < 2$, while for the standard BFKL it is $0 < \gamma_{BFKL} < 2$[‡]. We note that the authors of [37] also observed that the (analog of) the characteristic function in the frequency ordered approach is finite at $\gamma = 0$. The study in [37] was however done in the framework of a mixed equation that was perturbatively derived starting with NLO BFKL, and ostensibly contained some effects of nonlinear scattering as well as frequency evolution. The analog of characteristic function for negative values of γ was not studied in [37]. We therefore are not sure how to directly compare the two approaches and do not know whether the finiteness of $\chi(0)$ has the same physical origin in the approach of [37], although this is quite likely the case.

Given $\chi(\gamma)$ we have calculated the resulting scattering amplitude. As our study is numerical, we do not have a mathematical proof of analyticity of $\chi(\gamma)$. However comparison of the amplitude calculated as an integral along different curves in the complex plane strongly suggests that the function is analytic, as the results are identical within the range where our numerical calculation is stable. We have also shown that the numerical results are very well approximated by the saddle point integration.

The asymptotic saddle point is located at the point $\gamma_0^{BO} \approx -0.2$ with $\chi(\gamma_0^{BO}) \approx 2.89$. This again is very different from BFKL. where the asymptotic saddle point is located at $\gamma_0^{BFKL} = 1$ with $\chi(\gamma_0^{BFKL}) = 4\pi \ln 2 \approx 8.71$. The amplitude at asymptotically high energies is dominated by this saddle point, and thus the asymptotic solution of the BO-BFKL grows much slower - with one third of the rate - of the standard BFKL. The negative saddle point value for γ also means that the asymptotic amplitude in the BO-BFKL has anomalous dimension of $\gamma_0^{BO} \simeq -0.2$, and not $\gamma_0^{BFKL} = 1$ as in the standard BFKL.

We have also studied the saturation momentum using the method of [39]. In the simplest approximation scheme of [39] we find that the saturation momentum grows very slowly with energy, with the rate about six times smaller than in the BFKL with saturation boundary. Although this latter analysis is rather crude, in the BFKL framework it is know to give a good estimate of the actual result.

We thus arrive at the following picture. The frequency ordering which preserved energy conservation leads to a much slower growth of the amplitudes towards the saturation domain than predicted by the standard BFKL equation. Consistently, it gives a much slower growth of the saturation momentum with energy than in the standard BFKL/JIMWLK approach. This is rather disconcerting, as it suggests that one may have to wait until much higher energies than previously thought in order to see effects of saturation.

At this stage such conclusion is still premature, as our calculation in this paper is not complete. Here we have not included the DGLAP type splittings in the evolution. Instead we have assumed that

[‡]Note that our definition of γ differs by a factor of two from the commonly used one, see i.e. [41].

in all the kinematically allowed domain the emissions are generated by the eikonal vertex. Including the correct (DGLAP) kinematics for the splitting vertex close to the eikonal boundary (i.e. where longitudinal momenta of all three gluons entering/exiting the vertex are of the same order) is a little more complicated to do, but is the next natural step. We are currently working on this problem. It will be very interesting to see whether the more exact treatment of the splitting vertex can lead to a significant change in the picture of the evolution compared to our results in the present paper.

Acknowledgments

The research was supported by the Binational Science Foundation grant #2012124; MSCA RISE 823947 "Heavy ion collisions: collectivity and precision in saturation physics" (HIEIC), and by VATAT (Israel planning and budgeting committee) grant for supporting theoretical high energy physics. The work of H.D. and A.K. is supported by the NSF Nuclear Theory grant #2208387. The work of ML was funded by Binational Science Foundation grant #2021789 and by the ISF grant #910/23.
We thank Physics Departments of the Ben Gurion University and University of Connecticut for hospitality during mutual visits.
We also thank EIC Theory Institute, Brookhaven National Laboratory, CERN-TH group, National Centre for Nuclear Research, Warsaw; Institute for Nuclear Theory at the University of Washington, ECT*, and ITP at the University of Heidelberg for their support and hospitality during various stages of completing this project.

A Numerical procedure

Here we lay out the details of numerical calculation of eigenvalue $\chi(\gamma)$ for Eq. (2.32), where we use the form $f_\gamma(\boldsymbol{p}) = |\boldsymbol{p}|^\gamma$. Eq. (3.4) becomes,

$$\begin{aligned}
&\int_{\boldsymbol{p}^2>4\boldsymbol{q}^2} d^2\boldsymbol{p}\ \ \frac{\boldsymbol{q}^2}{\boldsymbol{p}^2(\boldsymbol{p}-\boldsymbol{q})^2}[|\boldsymbol{p}|^\gamma - \frac{1}{2}|\boldsymbol{q}|^\gamma] \\
&+\int_{(\boldsymbol{p}-\boldsymbol{q})^2>\boldsymbol{q}^2;\boldsymbol{p}^2<4\boldsymbol{q}^2} d^2\boldsymbol{p}\ \ \frac{1}{(\boldsymbol{p}-\boldsymbol{q})^2}\Big[1-2\frac{(\boldsymbol{p}-\boldsymbol{q})\cdot\boldsymbol{p}}{(\boldsymbol{p}-\boldsymbol{q})^2}\Theta((\boldsymbol{p}-\boldsymbol{q})^2-\boldsymbol{p}^2)\Big][|\boldsymbol{p}|^\gamma - \frac{1}{2}|\boldsymbol{q}|^\gamma] \\
&+\int_{\boldsymbol{q}^2<\boldsymbol{p}^2<4\boldsymbol{q}^2} d^2\boldsymbol{p}\ \ \frac{1}{\boldsymbol{p}^2}\Big[1-2\frac{(\boldsymbol{p}-\boldsymbol{q})\cdot\boldsymbol{p}}{(\boldsymbol{p}-\boldsymbol{q})^2}\Theta(\boldsymbol{p}^2-(\boldsymbol{p}-\boldsymbol{q})^2)\Big][|\boldsymbol{p}|^\gamma - \frac{1}{2}|\boldsymbol{q}|^\gamma] \\
&+\int_{\boldsymbol{p}^2<\boldsymbol{q}^2} d^2\boldsymbol{p}\frac{1}{\boldsymbol{p}^2}\Big(|\boldsymbol{p}+\boldsymbol{q}|^\gamma - |\boldsymbol{q}|^\gamma\Big) = \chi(\gamma)|\boldsymbol{q}|^\gamma
\end{aligned} \tag{A.1}$$

we denote,

$$\chi(\gamma) = \sum_i^6 \mathcal{I}_i \tag{A.2}$$

with $t \equiv \frac{|\boldsymbol{p}|}{|\boldsymbol{q}|}$, and ϕ to be the angle between $\boldsymbol{p}$ and $\boldsymbol{q}$. We then have,

$$\begin{aligned}
\mathcal{I}_1 =& \frac{1}{|\boldsymbol{q}|^\gamma}\int_{\boldsymbol{p}^2>4\boldsymbol{q}^2} d^2\boldsymbol{p}\ \ \frac{\boldsymbol{q}^2}{\boldsymbol{p}^2(\boldsymbol{p}-\boldsymbol{q})^2}[|\boldsymbol{p}|^\gamma - \frac{1}{2}|\boldsymbol{q}|^\gamma] \\
=& \int_0^{2\pi} d\phi \int_2^\infty \frac{dt}{t}\frac{t^\gamma - \frac{1}{2}}{t^2 - 2t\cos(\phi)+1}
\end{aligned} \tag{A.3}$$

Note that Θ functions can be applied as the limits of integration,

$$(\boldsymbol{p}-\boldsymbol{q})^2-\boldsymbol{p}^2>0\Rightarrow 1-2t\cos(\phi)>0 \tag{A.4}$$

and

$$(\boldsymbol{p}-\boldsymbol{q})^2-\boldsymbol{q}^2>0\Rightarrow t^2-2t\cos(\phi)>0 \tag{A.5}$$

Therefore,

$$\begin{aligned}\mathcal{I}_2=&\frac{1}{|\boldsymbol{q}|^\gamma}\int_{(\boldsymbol{p}-\boldsymbol{q})^2>\boldsymbol{q}^2;\boldsymbol{p}^2<4\boldsymbol{q}^2}\frac{d^2\boldsymbol{p}}{(\boldsymbol{p}-\boldsymbol{q})^2}[|\boldsymbol{p}|^\gamma-\frac{1}{2}|\boldsymbol{q}|^\gamma]\\=&\int_0^2 dt\int_{\arccos(\frac{t}{2})}^{2\pi-\arccos(\frac{t}{2})}d\phi\frac{t^{\gamma+1}-\frac{t}{2}}{t^2-2t\cos(\phi)+1}\end{aligned} \tag{A.6}$$

and

$$\begin{aligned}\mathcal{I}_3=&-2\frac{1}{|\boldsymbol{q}|^\gamma}\int_{(\boldsymbol{p}-\boldsymbol{q})^2>\boldsymbol{q}^2;\boldsymbol{p}^2<4\boldsymbol{q}^2}\frac{d^2\boldsymbol{p}}{(\boldsymbol{p}-\boldsymbol{q})^2}\Big(|\boldsymbol{p}|^\gamma-\frac{1}{2}|\boldsymbol{q}|^\gamma\Big)\Big[\frac{(\boldsymbol{p}-\boldsymbol{q})\cdot\boldsymbol{p}}{(\boldsymbol{p}-\boldsymbol{q})^2}\Theta((\boldsymbol{p}-\boldsymbol{q})^2-\boldsymbol{p}^2)\Big]\\=&-2\Big\{\int_0^1 dt\int_{\arccos(\frac{t}{2})}^{2\pi-\arccos(\frac{t}{2})}d\phi+\int_1^2 dt\int_{\arccos(\frac{1}{2t})}^{2\pi-\arccos(\frac{1}{2t})}d\phi\Big\}\frac{t^{\gamma+1}-\frac{t}{2}}{t^2-2t\cos(\phi)+1}\frac{t^2-t\cos(\phi)}{t^2-2t\cos(\phi)+1}\end{aligned} \tag{A.7}$$

and,

$$\begin{aligned}\mathcal{I}_4=&\frac{1}{|\boldsymbol{q}|^\gamma}\int_{\boldsymbol{q}^2<\boldsymbol{p}^2<4\boldsymbol{q}^2}d^2\boldsymbol{p}\ \ \frac{1}{\boldsymbol{p}^2}\Big[|\boldsymbol{p}|^\gamma-\frac{1}{2}|\boldsymbol{q}|^\gamma\Big]\\=&\int_0^{2\pi}d\phi\int_1^2\frac{dt}{t}(t^\gamma-\frac{1}{2})\end{aligned} \tag{A.8}$$

$$\begin{aligned}\mathcal{I}_5=&-\frac{2}{|\boldsymbol{q}|^\gamma}\int_{\boldsymbol{q}^2<\boldsymbol{p}^2<4\boldsymbol{q}^2}d^2\boldsymbol{p}\ \ \frac{1}{\boldsymbol{p}^2}\Big[\frac{(\boldsymbol{p}-\boldsymbol{q})\cdot\boldsymbol{p}}{(\boldsymbol{p}-\boldsymbol{q})^2}\Theta(\boldsymbol{p}^2-(\boldsymbol{p}-\boldsymbol{q})^2)\Big][|\boldsymbol{p}|^\gamma-\frac{1}{2}|\boldsymbol{q}|^\gamma]\\=&-4\int_1^2\frac{dt}{t}\int_0^{\arccos(\frac{1}{2t})}d\phi\frac{(t^\gamma-\frac{1}{2})(t^2-t\cos(\phi))}{t^2-2t\cos(\phi)+1}\end{aligned} \tag{A.9}$$

and

$$\begin{aligned}\mathcal{I}_6=&\frac{1}{|\boldsymbol{q}|^\gamma}\int_{\boldsymbol{p}^2<\boldsymbol{q}^2}d^2\boldsymbol{p}\frac{1}{\boldsymbol{p}^2}\Big(|\boldsymbol{p}+\boldsymbol{q}|^\gamma-|\boldsymbol{q}|^\gamma\Big)\\=&\int_0^{2\pi}d\phi\int_0^1\frac{dt}{t}\Big([t^2-2t\cos(\phi)+1]^{\frac{\gamma}{2}}-1\Big)\end{aligned} \tag{A.10}$$

These integrals only converge for certain range of γ. From the UV behavior, which we can extract from $\mathcal{I}_1$,

$$\begin{aligned}\mathcal{I}_1=&\int_0^{2\pi}d\phi\int_2^\infty\frac{dt}{t}\frac{t^\gamma-\frac{1}{2}}{t^2-2t\cos(\phi)+1}\\\approx&2\pi\int_2^\infty t^{\gamma-3}dt\end{aligned} \tag{A.11}$$

which requires $\gamma<2$, same as BFKL obviously. In practice, one introduce a UV cut-off Λ_{UV} for numerical evaluation. We choose $\Lambda_{UV}=10^8$. At our largest choice of $\gamma=1.8$, it's straightforward to estimate the error,

$$\int_{\Lambda_{UV}}^\infty\frac{dt}{t^{1.2}}=0.2\Lambda_{UV}^{-0.2}\Rightarrow 0.005 \tag{A.12}$$

On the other hand, there is also IR divergent terms $\mathcal{I}_2$ and $\mathcal{I}_4$, which put a lower limit on γ. They have the same level of divergence and to see them, we perform the angular integral first.

$$\begin{aligned}\mathcal{I}_2 &= \int_0^2 dt \int_{\arccos(\frac{t}{2})}^{2\pi-\arccos(\frac{t}{2})} d\phi \frac{t^{\gamma+1} - \frac{t}{2}}{t^2 - 2t\cos(\phi) + 1} \\ &= \int_0^2 dt \Big(t^{\gamma+1} - \frac{t}{2}\Big)\Big[\pi + \mathcal{O}(t)\Big]\end{aligned} \tag{A.13}$$

It's clear that the divergent behavior is dictated by the first term which is log divergent at $\gamma = -2$. It is the exact same analysis for $\mathcal{I}_6$, which we will not repeat there. At $\gamma_{min} = -1.8$, we then require a IR cut-off Λ_{IR},

$$\int_{\Lambda_{IR}}^2 dt\, t^{-0.8} \approx \Lambda_{IR}^{0.2} \tag{A.14}$$

with $\Lambda_{IR} = 10^{-8}$, $\Lambda_{IR}^{0.2} \sim 0.025$.

References

[1] H. Duan, A. Kovner, and M. Lublinsky, *Born-Oppenheimer renormalization group for high energy scattering: the formalism and the wave function*, arXiv:2412.05085.

[2] H. Duan, A. Kovner, and M. Lublinsky, *Born-Oppenheimer renormalization group for high energy scattering: the CSS, the DGALP and all that*, arXiv:2412.05097.

[3] J. Collins, *Foundations of Perturbative QCD*, vol. 32 of *Camb.Monogr.Part.Phys.Nucl.Phys.Cosmol.* Cambridge University Press, 2011.

[4] J. C. Collins and D. E. Soper, *Parton distribution and decay functions*, *Nucl. Phys. B* **193** (1981) 381. [Erratum-ibid. B 213, 545 (1983)].

[5] J. C. Collins and D. E. Soper, *Back-to-back jets in qcd*, *Nucl. Phys. B* **197** (1982) 446.

[6] J. C. Collins, D. E. Soper, and G. Sterman, *Factorization of hard processes in qcd*, *Nucl. Phys. B* **250** (1985) 199.

[7] I. Balitsky, *Operator expansion for high-energy scattering*, *Nucl. Phys. B* **463** (1996) 99–160, [hep-ph/9509348].

[8] I. Balitsky, *Factorization for high-energy scattering*, *Phys. Rev. Lett.* **81** (1998) 2024–2027, [hep-ph/9807434].

[9] I. Balitsky, *Factorization and high-energy effective action*, *Phys. Rev. D* **60** (1999) 014020, [hep-ph/9812311].

[10] J. Jalilian-Marian, A. Kovner, A. Leonidov, and H. Weigert, *The wilson renormalization group for low x physics: Gluon evolution at finite parton density*, *Nucl. Phys. B* **504** (1997) 415–431, [hep-ph/9709432].

[11] J. Jalilian-Marian, A. Kovner, A. Leonidov, and H. Weigert, *The wilson renormalization group for low x physics: Towards the high density regime*, *Phys. Rev. D* **59** (1998) 014014, [hep-ph/9706377].

[12] J. Jalilian-Marian, A. Kovner, and H. Weigert, *The wilson renormalization group for low x physics: Gluon evolution at finite parton density*, *Phys. Rev. D* **59** (1998) 014015, [hep-ph/9709432].

[13] A. Kovner and J. G. Milhano, *High energy evolution in perturbative qcd beyond leading logarithms*, *Phys. Rev. D* **61** (2000) 014012, [hep-ph/9904420].

[14] A. Kovner, J. G. Milhano, and H. Weigert, *Relating different approaches to nonlinear qcd evolution at finite gluon density*, *Phys. Rev. D* **62** (2000) 114005, [hep-ph/0004014].

[15] H. Weigert, *Unitarity at small x*, *Nucl. Phys. A* **703** (2002) 823–860, [hep-ph/0004044].

[16] E. Iancu, A. Leonidov, and L. McLerran, *Nonlinear gluon evolution in the color glass condensate: I*, *Nucl. Phys. A* **692** (2001) 583–645, [hep-ph/0011241].

[17] E. Iancu, A. Leonidov, and L. McLerran, *The renormalization group equation for the color glass condensate*, *Phys. Lett. B* **510** (2001) 133–144, [hep-ph/0102009].

[18] E. Ferreiro, E. Iancu, A. Leonidov, and L. McLerran, *Nonlinear gluon evolution in the color glass condensate: Ii*, *Nucl. Phys. A* **703** (2002) 489–538, [hep-ph/0109115].

[19] A. Kovner, M. Lublinsky, and Y. Mulian, *Jalilian-Marian, Iancu, McLerran, Weigert, Leonidov, Kovner evolution at next to leading order*, *Phys. Rev. D* **89** (2014), no. 6 061704, [1310.0378 [hep-ph]].

[20] A. Kovner, M. Lublinsky, and Y. Mulian, *NLO JIMWLK Evolution Unabridged*, *JHEP* **08** (2014) 114, [arXiv:1405.0418].

[21] M. Lublinsky and Y. Mulian, *High energy QCD at NLO: from light-cone wave function to JIMWLKevolution*, *JHEP* **05** (2017) 097, [arXiv:1610.03453].

[22] V. S. Fadin, E. A. Kuraev, and L. N. Lipatov, *On the Pomeranchuk singularity in asymptotically free Theories*, *Phys. Lett. B* **60** (1975) 50.

[23] V. S. Fadin, E. A. Kuraev, and L. N. Lipatov, *The Pomeranchuk singularity in QCD*, *Sov. Phys. JETP* **45** (1977) 199.

[24] Y. Y. Balitsky and L. N. Lipatov, *The Pomeranchuk singularity in QCD and QED*, *Sov. J. Nucl. Phys.* **28** (1978) 22.

[25] V. S. Fadin and L. N. Lipatov, *BFKL Pomeron in the next-to-leading Approximation*, *Phys. Lett. B* **429** (1998) 127–134, [hep-ph/9802290].

[26] G. Camici and M. Ciafaloni, *Energy scale(s) and next-to-leading bfkl equation*, *Phys. Lett. B* **430** (1998) 349–354, [hep-ph/9803389].

[27] G. Salam, *A resummation of large subleading corrections at small x*, *JHEP* **9807** (1998) 019, [hep-ph/9806482].

[28] M. Ciafaloni and D. Colferai, *The bfkl equation at next-to-leading level and beyond*, *Phys. Lett. B* **452** (1999) 372–378, [hep-ph/9812366].

[29] M. Ciafaloni, D. Colferai, and G. Salam, *Renormalization group improved small x equation*, *Phys. Rev. D* **60** (1999) 114036, [hep-ph/9905566].

[30] M. Ciafaloni, D. Colferai, G. Salam, and A. Stasto, *Renormalization group improved small x green's function*, *Phys. Rev. D* **68** (2003) 114003, [hep-ph/0307188].

[31] A. S. Vera, *An 'all-poles' approximation to collinear resummations in the regge limit of perturbative qcd*, *Nucl. Phys. B* **722** (2005) 65–80, [hep-ph/0505128].

[32] T. Lappi and H. Mäntysaari, *Direct numerical solution of the coordinate space Balitsky-Kovchegov equation at next to leading order*, *Phys. Rev. D* **91** (2015), no. 7 074016, [arXiv:1502.02400].

[33] K. Kutak and A. M. Staśto, *Unintegrated gluon distribution from modified BK equation*, *Eur. Phys. J. C* **41** (2005) 343–351, [hep-ph/0408117].

[34] L. Motyka and A. M. Staśto, *Exact kinematics in the small x evolution of the color dipole and gluon cascade*, *Phys. Rev. D* **79** (2009) 085016, [arXiv:0901.4949].

[35] G. Beuf, *Improving the kinematics for low-x QCD evolution equations in coordinate space*, *Phys. Rev. D* **89** (2014), no. 7 074039, [arXiv:1401.0313].

[36] E. Iancu, J. D. Madrigal, A. H. Mueller, G. Soyez, and D. N. Triantafyllopoulos, *Collinearly-improved BK evolution meets the HERA data*, *Phys. Lett. B* **750** (2015) 643–652, [arXiv:1507.03651].

[37] B. Ducloué, E. Iancu, A. H. Mueller, G. Soyez, and D. N. Triantafyllopoulos, *Non-linear evolution in QCD at high-energy beyond leading order*, *JHEP* **04** (2019) 081, [arXiv:1902.06637].

[38] A. Kovner, M. Lublinsky, V. Skokov, and Z. Zhao, *Not all that is β_0 is β-function: the DGLAP resummation and the running coupling in NLO JIMWLK*, *JHEP* **07** (2024) 148, [2308.15545].

[39] A. H. Mueller and D. N. Triantafyllopoulos, *The energy dependence of the saturation momentum*, *Nucl. Phys. B* **640** (2002) 331–350, [hep-ph/0205167].

[40] A. Kovner, M. Lublinsky, and U. Wiedemann, *From bubbles to foam: Dilute to dense evolution of hadronic wave function at high energy*, *JHEP* **06** (2007) 075, [arXiv:0705.1713].

[41] Y. Kovchegov and E. Levin, *Introduction to High Energy QCD*. Cambridge University Press, 2012.